

Stochastic leverage effect in high-frequency data: a Fourier based analysis.

Imma Valentina Curato*and Simona Sanfelici†

March 11, 2022

Abstract

We analyse the stochastic leverage effect, which is defined as the instantaneous correlation between the returns and their related volatility increments, in a stochastic volatility model set-up. We define a novel estimator of the effect which is based on a pre-estimation of the Fourier coefficients of the return and of the volatility process as defined in Malliavin and Mancino (2002). We establish the consistency of the estimator and we analyse its finite sample performance in the presence of microstructure noise contamination. When applying our methodology to real data, our results provide evidence of the presence of the stochastic leverage effect.

JEL Classification: C13, C14, C51, C58

Keywords: Fourier analysis, leverage effect, high-frequency data, microstructure noise

1 Introduction

The leverage effect is one of the most striking empirical regularity observed in the financial time series. In its classical interpretation given by Black [8] and Christie [14], the effect refers to the negative and constant correlation typically observed between returns and their respective volatilities. The papers [7, 10, 11, 17, 18, 19, 31] and [36] are a non exhaustive list of the empirical works investigating the presence of constant and negative correlation between returns and volatilities across different financial asset types. The authors observe that the effect is in general larger for aggregate market index returns than for individual stocks, see discussion in [33], and detectable at frequencies lower than or equal to 1 day. For high-frequency data, i.e. intra-daily data, not all the empirical works in the literature find consensus in interpreting the leverage effect as above. In fact, there are studies which indeed demonstrate the presence of a

*Corresponding author: Ulm University, Institute of Mathematical Finance, Helmholtzstrae 18, 89069 Ulm, Germany. E-MAIL: imma.curato@uni-ulm.de

†University of Parma, Department of Economics, Via J. Kennedy, 6, 43125 Parma, Italy. E-MAIL: simona.sanfelici@unipr.it

constant and negative correlation between returns and volatilities, see [2, 9, 33] and also others which support the claim of a time-varying [4, 18, 37], or itself stochastic correlation between returns and volatilities [1, 3, 12, 22, 28, 29, 30].

In a high-frequency framework, it is then more appropriate to interpret the leverage effect as in Aït Sahalia et al. [2], i.e. as the instantaneous correlation between returns and the increments of their volatilities. This definition also allows us to obtain an easy interpretation of the effect in a stochastic volatility model set-up. More precisely, let the logarithmic asset price p and the volatility process σ^2 be a solution to the system of equations

$$\begin{cases} dp(t) &= a(t) dt + \sigma(t) dW(t) \\ d\sigma^2(t) &= b(t) dt + \gamma(t) dZ(t) \end{cases} \quad (1)$$

where $W(t)$, $t \geq 0$ and $Z(t)$, $t \geq 0$ are two correlated standard Brownian motions defined on the probability space $(\Omega, \mathcal{F}, \mathbb{P})$. The correlation process is defined as $\rho(t)$ with values in $[-1, 1]$. The *stochastic leverage effect* is defined as

$$R(t) = \frac{\langle dp(t), d\sigma^2(t) \rangle}{\sqrt{\langle dp(t), dp(t) \rangle \langle d\sigma^2(t), d\sigma^2(t) \rangle}}, \quad (2)$$

where the instantaneous quadratic covariation between the returns and the volatility increments and the instantaneous quadratic variation of the returns and of the volatility increments appear at the numerator and denominator, respectively. The model setup (1) encompasses parametric models as, for instance, the Heston model [21] and the generalized Heston model presented in [35]. If the leverage effect is present then $\rho(t)$ is modelled as a negative constant in the Heston model and as a Jacobi process with values in $[-1, 1]$ in the generalized Heston model. Moreover, for the former model $R(t) = \rho$ and for the latter $R(t)$ is a stochastic process with values in $[-1, 1]$.

An estimation procedure for (2) can be found in Aït Sahalia et al. [2] under the assumption that p and σ^2 follow a Heston model with stationary volatility. In this special case, the authors observe that at high frequency and over a short horizon the estimation of $R(t)$ is close to zero instead of being a strongly negative value, whereas the leverage effect is present when looking at longer horizons. In [2], the authors discuss this estimation puzzle and show that the problem relies on the proxy employed in place of the unobservable volatility path. This means that, typically, an estimation of $R(t)$ is affected by different sources of bias which makes its estimation difficult. Different proxies can be employed to overcome the aforementioned puzzle, like local averages of integrated volatility estimators as suggested in [2], the CBOE volatility index (VIX), or the Black Scholes implied volatility [22].

An alternative measure of the leverage effect at high frequency can be defined as the scaled

quadratic covariation between p and σ^2 in a time window $[0, T]$, see [3, Formula 8.42] and [22],

$$R_T = \frac{\langle p(t), \sigma^2(t) \rangle_T}{\sqrt{\langle p(t), p(t) \rangle_T \langle \sigma^2(t), \sigma^2(t) \rangle_T}} = \frac{\int_0^T \sigma(t) \gamma(t) \rho(t) dt}{\sqrt{\int_0^T \sigma^2(t) dt \int_0^T \gamma^2(t) dt}}, \quad (3)$$

where the quadratic variation of p and of σ^2 appear at the denominator. For instance, if we assume that p and σ^2 follow an Heston model then $R_T = \rho$, otherwise R_T is a random quantity.

Estimators of R_T can be found in [1] and [3] where the authors employ realized covariance-based estimators. However, they do not investigate the finite sample properties of their estimations in the presence of microstructure noise contamination which typically appears in data at frequencies higher than 5 minutes, e.g. when tick-data are at disposal. In fact, if the data are sampled at sufficiently high-frequency, asset prices tend to incorporate the mechanism of the trading process such as bid/ask bounces, the different price impact of different types of trades, limited liquidity, or other types of frictions.

In this paper, we define an estimator of R_T in the modelling set-up (1) based on the use of the Fourier methodology introduced in [24], see also [26] for a complete overview, and we study its finite sample performance in the presence of microstructure noise. We call it the *Fourier estimator of the stochastic leverage effect*. As its name suggests, our estimation procedure is completely defined in the frequency domain. This procedure allows us to overcome the bias due to the unobservable volatility path in the estimation. In order to define a Fourier estimator of R_T , we then combine together three different estimators: the Fourier estimator of the integrated leverage effect (FEL in short), the Fourier estimator of the integrated volatility (FEV in short) and of the integrated volatility of volatility (FEVV in short) which have been defined in [16], [24] and [32], respectively. This also means that our methodology still works when non-equidistant data are at disposal, without the need of manipulating the data or changing the set-up of the estimation methodology.

When estimating second order latent quantities as the quadratic covariation between logarithmic price and volatility or the quadratic variation of the volatility in $[0, T]$, we handle the latency of the volatility by computing N Fourier coefficients of the volatility process. This is a step that requires the preliminary computation of M Fourier coefficients of the returns. We call the parameters M and N *cutting frequencies* in the following.

We start by developing an estimation strategy in the absence of microstructure noise. Thus, p is the underlying efficient logarithmic price process. The choice of a continuous-time modelling setup for p is driven by the empirical work [13] where the authors highlight that the jump variation computed from tick data is an order of magnitude smaller than the consensus view in the literature that uses five-minute or lower-frequency data. This means that our ability to distinguish true discrete jumps from continuous diffusive variation diminishes as we increase the sampling frequency. For example, a short-lived burst of volatility is likely to be identified as a jump when working with data sampled at a frequency lower than 5 minutes but it is com-

patible with a continuous path when working with tick-data. This said, the Fourier estimation methodology, that we present, is suitable when data at frequencies higher than 5 minutes are at disposal.

To show the consistency of the Fourier estimator of the stochastic leverage effect, we first analyse the conditions under which the FEL, the FEV, and the FEVV are consistent. Let $\mathcal{S}_n := \{0 = t_0 \leq t_1 \leq \dots \leq t_n = T\}$, for all $i = 0, \dots, n$, and define $\tau(n) = \max_{i=0, \dots, n-1} |t_{i+1} - t_i|$. Among the assumptions under which the consistency of the FEV and the FEVV is proven we find that $M\tau(n) \rightarrow 0$ as $n, M \rightarrow \infty$ and $\tau(n) \rightarrow 0$. However, under this assumption, it does not exist in the literature a proof of consistency for the FEL. We show that the FEL is consistent under the assumption above, which is not considered in [15, 16], and then give a formal definition of R_T and show its consistency.

We then add independent noise to the underlying efficient price process dynamics. The finite sample properties of the FEV have been analysed in the presence of microstructure noise contamination in [27] whereas the ones of the FEVV are analysed in [32]. For the FEL, an analysis of its asymptotic properties is conducted in [15] and [16] but not a study of its finite sample properties in the presence of microstructure noise contamination. We then analyse in this paper the behaviour of the bias and the mean squared error of the FEL. The estimator is asymptotically unbiased but it shows a diverging mean squared error. The increase of variance in the presence of microstructure noise contamination is a phenomenon already observed for integrated estimators in a high-frequency setting. For example, the variance of the realized variance estimator diverges in the presence of microstructure noise contamination as analysed in [5]. In this framework, see [3] for a complete review, the presence of microstructure noise is usually handled by using the pre-averaging approach as discussed in [23]. This is also the approach used in [1] and [29] to define estimators of the integrated leverage effect robust to microstructure noise contamination. However, the Fourier approach is designed to filter the noise components on its own without resorting to manipulations of the original data set, see discussion in [26, Chapter 5]. Therefore, correcting our estimation by using a pre-averaging approach is not an option. On the other hand, we can determine an optimal selection procedure for the cutting frequency parameters M and N to balance the contrasting effects observed in the finite sample bias and variance of the estimator. By using Monte-Carlo data sets drawn by the Heston [21] and the generalized Heston model [35], we analyse the performance of an optimal selection strategy of the parameters M and N based on the minimization of the sample variance of the estimator. Moreover, we define a variance corrected estimator of the FEL in the presence of microstructure noise to further reduce the variance of the estimator. The optimal parameters M and N obtained by using the latter estimator will typically reduce the sample variance of the estimation by a half. Considering the estimator of the integrated leverage effect of Mykland and Wang [29] as a benchmark of the FEL, we show a comparison between the two estimators on data generated by the Heston model, we also show a comparison between this estimator and the FEL. At last, we perform a sensitivity analysis on the FEL on data sets generated from the generalized Heston model.

We finally have all the ingredients to define a Fourier-based estimation strategy of the stochastic leverage effect in the presence of microstructure noise contamination which is discussed in Section 4.

The remainder of the paper is organized as follows. In Section 2, we introduce the model set-up, the definition of the FEL, and of the Fourier estimator of the stochastic leverage effect together with their asymptotic properties in the absence of microstructure noise. In Section 3, we analyse the finite sample properties of the FEL in the presence of microstructure noise and an optimal selection strategy for its related cutting frequencies parameters. In Section 4, we discuss how to practically implement the Fourier estimator of the stochastic leverage effect in the presence of microstructure noise contamination. Section 5 applies our results to real financial data. The Appendix contains the proofs of all statements presented in the paper.

2 Estimation of the stochastic leverage effect in the absence of microstructure

We perform our analysis in a time window $[0, T]$ for all $T > 0$, and such that the processes appearing in the underlying efficient price process (1) satisfy the following assumption:

- **(H1)** $a(t)$, $b(t)$, $\sigma(t)$, $\gamma(t)$ and $\rho(t)$ are \mathbb{R} -valued processes, almost surely continuous on $[0, T]$ and adapted to the filtration \mathcal{F} such that

$$\begin{aligned} \mathbb{E} \left[\sup_{t \in [0, T]} |a(t)|^8 \right] < \infty, \quad \mathbb{E} \left[\sup_{t \in [0, T]} |b(t)|^8 \right] < \infty, \\ \mathbb{E} \left[\sup_{t \in [0, T]} |\sigma(t)|^8 \right] < \infty, \quad \mathbb{E} \left[\sup_{t \in [0, T]} |\gamma(t)|^8 \right] < \infty, \\ \mathbb{E} \left[\sup_{t \in [0, T]} |\rho(t)|^8 \right] < \infty. \end{aligned}$$

2.1 Fourier estimator of the integrated leverage effect

Let us first introduce the Fourier estimator of the integrated leverage effect as defined in [15, 16].

We define the leverage process $\eta(t)$ as

$$\langle dp(t), d\sigma^2(t) \rangle = \sigma(t)\gamma(t)\rho(t)dt = \eta(t)dt, \tag{4}$$

and we are interested in estimating the integrated covariation between the logarithmic price p and the volatility process σ^2 , which appears at the numerator of (3), by determining an estimator for

$$\eta = \int_0^T \eta(t)dt. \tag{5}$$

To this aim, we need to define the Fourier coefficients of the leverage process. Following [24], we define the Fourier coefficients of the returns and of the increments of the volatility process as

$$c(l; dp) = \frac{1}{T} \int_0^T e^{-i\frac{2\pi}{T}lt} dp(t), \quad (6)$$

and

$$c(l; d\sigma^2) = \frac{1}{T} \int_0^T e^{-i\frac{2\pi}{T}lt} d\sigma^2(t), \quad (7)$$

for each $l \in \mathbb{Z}$.

Given two functions Φ and Ψ on the integers \mathbb{Z} , we say that their Bohr convolution product exists if the following limit exists for all integers h

$$(\Phi * \Psi)(h) := \lim_{N \rightarrow \infty} \frac{1}{2N+1} \sum_{|l| \leq N} \Phi(l) \Psi(h-l).$$

Under Assumptions (H1), let $(p(t), \sigma^2(t))$ be a solution of (1). For a fixed h , we define $\Phi(l) := c(l; d\sigma^2)$ and $\Psi(h-l) := c(h-l, dp)$, then the limit in probability of the Bohr convolution product exists and converges to the h -th Fourier coefficient of the leverage process. This result immediately follows from [25, Theorem 2.1]. The h -th Fourier coefficient of $\eta(t)$ is then

$$c(h; \eta) = \lim_{N \rightarrow \infty} \frac{T}{2N+1} \sum_{|l| \leq N} c(l; d\sigma^2) c(h-l; dp) = \frac{1}{T} \int_0^T e^{-i\frac{2\pi}{T}ht} \eta(t) dt. \quad (8)$$

The identity above has the obvious drawback to being feasible only when continuous observations of the logarithmic price and of the volatility paths are available.

We now introduce the normalized Dirichlet kernel $D_N(t)$

$$D_N(t) = \frac{1}{2N+1} \sum_{|l| \leq N} e^{i\frac{2\pi}{T}lt}, \quad (9)$$

and its first derivative $D'_N(t)$

$$D'_N(t) = \frac{1}{2N+1} \sum_{|l| \leq N} il \frac{2\pi}{T} e^{i\frac{2\pi}{T}lt} \quad (10)$$

which are going to be extensively used in the following. We also remind the reader that the following results hold.

Proposition 2.1. *Let $D_N(t)$ be the normalized Dirichlet kernel defined in (9), then the following properties are satisfied.*

1. $\int_0^T |D_N(u)|^2 du = \frac{T}{2N+1}$,
2. $\forall p > 1$, there exists a constant \mathcal{C}_p such that $\int_0^T |D_N(u)|^p du = \frac{\mathcal{C}_p}{2N+1}$.

Let us assume that we can continuously observe the logarithmic price paths and that the volatility paths are unobservable.

For all $l \neq 0$, by means of the use of the integration by parts formula, we have that

$$c(l; d\sigma^2) = il \frac{2\pi}{T} c(l; \sigma^2) + \frac{1}{T} (\sigma^2(T) - \sigma^2(0)), \quad (11)$$

where

$$c(l; \sigma^2) = \frac{1}{T} \int_0^T e^{-i\frac{2\pi}{T}lt} \sigma^2(t) dt.$$

Therefore, the limit (8) becomes

$$\begin{aligned} c(h; \eta) &= \lim_{N \rightarrow \infty} \frac{T}{2N+1} \sum_{|l| \leq N} \left(il \frac{2\pi}{T} c(l; \sigma^2) + \frac{1}{T} (\sigma^2(T) - \sigma^2(0)) \right) c(h-l; dp) \\ &= \lim_{N \rightarrow \infty} \frac{T}{2N+1} \sum_{|l| \leq N} il \frac{2\pi}{T} c(l; \sigma^2) c(h-l; dp) + \frac{T}{2N+1} \sum_{|l| \leq N} \frac{1}{T} (\sigma^2(T) - \sigma^2(0)) c(h-l; dp) \\ &= \lim_{N \rightarrow \infty} \frac{1}{T} \int_0^T \int_0^T e^{-i\frac{2\pi}{T}ht} D'_N(t-s) \sigma^2(s) ds dp(t) + \frac{1}{T} \int_0^T (\sigma^2(T) - \sigma^2(0)) e^{-i\frac{2\pi}{T}ht} D_N(t) dp(t). \end{aligned}$$

The second summand converges to 0 in probability as N tends to infinity. In fact, by applying the Itô isometry and the Cauchy-Schwartz inequality

$$\mathbb{E} \left[\left| \frac{1}{T} \int_0^T (\sigma^2(T) - \sigma^2(0)) e^{-i\frac{2\pi}{T}ht} D_N(t) dp(t) \right|^2 \right] \leq C \frac{T}{2N+1}$$

because of Proposition 2.1 and Assumption (H1), where C is a constant independent of N .

Thus,

$$c(h; \eta) = \lim_{N \rightarrow \infty} \frac{T}{2N+1} \sum_{|l| \leq N} i \frac{2\pi}{T} l c(l; \sigma^2) c(h-l; dp) \quad (12)$$

In order to construct an estimation procedure for the h -th Fourier coefficient of the leverage process, we consider the truncation of the limit in (12) and obtain

$$c_N(h; \eta) = \frac{T}{2N+1} \sum_{|l| \leq N} i \frac{2\pi}{T} l c(l; \sigma^2) c(h-l; dp) \quad (13)$$

where only the Fourier coefficients of the return and of the volatility process appear.

We now assume to observe $p(t)$ on a discrete non-equidistant time grid

$$\mathcal{S}_n := \{0 = t_0 \leq t_1 \leq \dots \leq t_n = T\}, \quad \text{for all } i = 0, \dots, n,$$

and that the volatility paths are unobservable. We define $\tau(n) := \max_{i=0, \dots, n-1} |t_{i+1} - t_i|$ and the discrete observed return as $\delta_i = p(t_{i+1}) - p(t_i)$ for all $i = 0, \dots, n-1$.

Following [15, 16], an estimator of the h -th Fourier coefficient of the leverage process can

be defined as

$$c_{n,M,N}(h; \eta) = \frac{T}{2N+1} \sum_{|l| \leq N} il \frac{2\pi}{T} c_{n,M}(l; \sigma^2) c_n(h-l; dp), \quad (14)$$

for any integer h such that $|h| \leq N$, where $c_n(s; dp)$ are the discrete Fourier coefficients of the returns

$$c_n(s; dp) = \frac{1}{T} \sum_{i=0}^{n-1} e^{-is \frac{2\pi}{T} t_i} \delta_i(p) \quad (15)$$

for $|s| \leq N+M$ and $c_{n,M}(h; \sigma^2)$ are the Fourier coefficients of the volatility process introduced in [24] for $|l| \leq N$

$$c_{n,M}(l; \sigma^2) = \frac{T}{2M+1} \sum_{|s| \leq M} c_n(s; dp) c_n(l-s; dp). \quad (16)$$

The above-mentioned estimators are written as functions of n , M , and N which stand for the number of observations available, the number of the discrete Fourier coefficients of the returns, and of the Fourier coefficients of the volatility process as defined in (16), respectively.

Finally, the Fourier estimator of the integrated leverage effect (FEL) is an estimator of (5) and is obtained by definition (14) for $h = 0$

$$\hat{\eta}_{n,M,N} = T c_{n,M,N}(0; \eta) = \frac{T^2}{2N+1} \sum_{|l| \leq N} il \frac{2\pi}{T} c_{n,M}(l; \sigma^2) c_n(-l; dp).$$

We can also give a more explicit form of the estimator by employing D_M and D'_N as defined in (9) and (10)

$$\hat{\eta}_{n,M,N} = \sum_{i=0}^{n-1} \sum_{j=0}^{n-1} \sum_{k=0}^{n-1} D_M(t_i - t_j) D'_N(t_k - t_j) \delta_i \delta_j \delta_k. \quad (17)$$

In [16], it is shown that the estimator (17), in the absence of microstructure noise, is consistent if $N^2/M \rightarrow 0$ and $M\tau(n) \rightarrow a$ with $a > 0$ as n, M, N goes to infinity and $\tau(n)$ goes to zero. We prove now a consistency result under a different set of assumptions. This is a necessary preliminary step to define a consistent estimator for R_T as it will be clearer in Section 2.2.

Theorem 2.2. *We assume that Assumption (H1) and*

$$\frac{N^2}{M} \rightarrow 0 \quad \text{and} \quad MN\tau(n) \rightarrow 0 \quad (18)$$

hold true as $n, M, N \rightarrow \infty$ and $\tau(n) \rightarrow 0$. Then

$$\hat{\eta}_{n,M,N} \xrightarrow{\mathbb{P}} \eta. \quad (19)$$

Remark 2.3. *In the proof of Theorem 2.2, see the Appendix, it is shown that the drift components of the logarithmic price and of the volatility process are negligible in probability with respect to the diffusive components. For simplicity, we will then assume throughout the paper that the*

drift terms $a(t)$ and $b(t)$ in the model (1) are equal to zero.

2.2 Fourier estimator of the stochastic leverage effect

We can now define an estimator of R_T by combining the FEL, the FEV and the FEVV as defined in (17), [24] and [32], respectively,

$$\hat{R}_T = \frac{\hat{\eta}_{n,M,M}}{\sqrt{\hat{\sigma}_{n,M}^2 \hat{\gamma}_{n,M,N}^2}}$$

where

$$\hat{\sigma}_{n,M}^2 = \frac{T^2}{2M+1} \sum_{|s| \leq M} c_n(s; dp) c_n(-s; dp) \quad (20)$$

and

$$\hat{\gamma}_{n,M,N}^2 = \lim_{N \rightarrow \infty} \frac{T^2}{2N+1} \sum_{|l| \leq N} \left(1 - \frac{|l|}{N}\right) l^2 \frac{4\pi^2}{T^2} c_{n,M}(l; \sigma^2) c_{n,M}(-l; \sigma^2). \quad (21)$$

In the definition of (21), the Barlett kernel improves the performance of the estimator when very high-frequency observations are used. In conclusion, we can prove the consistency of the estimator R_T by simply using the continuous mapping theorem.

Theorem 2.4. *We assume that Assumption (H1) and*

$$\frac{N^4}{M} \rightarrow 0 \quad \text{and} \quad MN\tau(n) \rightarrow 0$$

hold true as $n, M, N \rightarrow \infty$ and $\tau(n) \rightarrow 0$. Then

$$\hat{R}_T \xrightarrow{\mathbb{P}} R_T.$$

Remark 2.5. *Analysing the asymptotic distribution of the estimation error of \hat{R}_T is outside the scope of this paper. Different estimators of R_T can be found in [1, Section 7.5] but also in this case the asymptotic properties of the estimators are not further discussed. Broadly speaking, having once shown that central limit results hold for the estimators of the integrated leverage effect, the integrated volatility and the integrated volatility of volatility under the same set of assumptions, asymptotic limit results can be simply obtained by using the delta method.*

3 Finite sample properties of the Fourier estimator of the integrated leverage effect

The finite sample properties of the FEV and the FEVV have been analysed in the presence of microstructure noise in [27] and [32], respectively. With the aim of defining an estimation of R_T

in the presence of microstructure noise, we need to analyse first the finite sample properties of the FEL under microstructure noise contamination.

We add microstructure noise contamination to the underlying efficient log-price $p(t)$ defined in (1) by assuming that the logarithm of the observed price is

$$\tilde{p}(t_i) = p(t_i) + \zeta(t_i) \quad (22)$$

where $\zeta(t)$ is the microstructure noise.

We make the following assumption

- **(H2)** The random shocks $(\zeta(t_i))_{0 \leq i \leq n}$, for all n , are independent and identically distributed with bounded sixth moment. Moreover, the random shocks are independent of the efficient price process p .

We define $\epsilon_i = \zeta(t_{i+1}) - \zeta(t_i)$ and $\tilde{\delta}_i = \tilde{p}(t_{i+1}) - \tilde{p}(t_i)$. Then, the FEL (17) in the presence of microstructure noise becomes

$$\tilde{\eta}_{n,M,N} = \sum_{i=0}^{n-1} \sum_{j=0}^{n-1} \sum_{k=0}^{n-1} D_M(t_i - t_j) D'_N(t_k - t_j) \tilde{\delta}_i \tilde{\delta}_j \tilde{\delta}_k. \quad (23)$$

We can disentangle (23) in the following components

$$\sum_{i \neq j \neq k} D_M(t_i - t_j) D'_N(t_k - t_j) \tilde{\delta}_i \tilde{\delta}_j \tilde{\delta}_k \quad (24)$$

$$\begin{aligned} &+ \sum_{i,j:i \neq j} D_M(t_i - t_j) D'_N(t_i - t_j) \tilde{\delta}_i^2 \tilde{\delta}_j + \sum_{i,j} D'_N(t_i - t_j) \tilde{\delta}_i \tilde{\delta}_j^2 \\ &= \sum_{i \neq j \neq k} D_M(t_i - t_j) D'_N(t_k - t_j) \delta_i \delta_j \delta_k \end{aligned} \quad (25)$$

$$+ \sum_{i,j:i \neq j} D_M(t_i - t_j) D'_N(t_i - t_j) \delta_i^2 \delta_j + \sum_{i,j} D'_N(t_i - t_j) \delta_i \delta_j^2 \quad (26)$$

$$+ \eta_{n,M,N}^\epsilon,$$

where the sum of the components (25) and (26) correspond to the FEL in the absence of microstructure noise contamination (17) and

$$\begin{aligned} \eta_{n,M,N}^\epsilon &= \sum_{i,j,k:i \neq j \neq k} D_M(t_i - t_j) D'_N(t_k - t_j) (\delta_i \delta_j \epsilon_k + \delta_j \delta_k \epsilon_i + \delta_k \delta_i \epsilon_j + \delta_i \epsilon_j \epsilon_k + \delta_j \epsilon_i \epsilon_k + \delta_k \epsilon_i \epsilon_j + \epsilon_i \epsilon_j \epsilon_k) \\ &+ \sum_{i,j:i \neq j} D_M(t_i - t_j) D'_N(t_i - t_j) (\delta_i \epsilon_j + \epsilon_i^2 \delta_j + \epsilon_i^2 \epsilon_j + 2\delta_i \delta_j \epsilon_i + 2\delta_i \epsilon_j \epsilon_i) \\ &+ \sum_{i,j} D'_N(t_i - t_j) (\delta_j \epsilon_i + \epsilon_j^2 \delta_i + \epsilon_j^2 \epsilon_i + 2\delta_j \delta_i \epsilon_j + 2\delta_j \epsilon_i \epsilon_j). \end{aligned}$$

We remind the reader that the integrated leverage effect under the modelling assumption (1) can be positive or negative. Therefore, we analyse the bias of the estimator in absolute value. The definition of the FEL does not require the use of equidistant data. Anyway for simplicity of computation, we assume to observe equidistant data in the time window $[0, T]$ and that $\frac{T}{n}$ is the distance between two observations. Moreover, we consider throughout the section, that the drift components of the underlying model (1) are zero, following Remark 2.3.

Theorem 3.1. *We assume that (H1), (H2) and*

$$\frac{N^2}{M} \rightarrow 0 \quad \text{and} \quad \frac{MN}{n} \rightarrow 0 \quad (27)$$

hold true as $N, M, n \rightarrow \infty$ and $n \rightarrow \infty$, then the estimator $\tilde{\eta}_{n,M,N}$ is asymptotically unbiased. More precisely,

$$\begin{aligned} \left| \mathbb{E}[\tilde{\eta}_{n,M,N} - \eta] \right| &\leq \left| \mathbb{E}[\eta_{n,M,N} - \int_0^T \eta(t) dt] \right| + \left| \mathbb{E}[\eta_{n,M,N}^\epsilon] \right| \\ &\leq \Gamma(n, M, N) + \Lambda(n, N) + \Psi(N) + o(1) + \left| 2(n-1) \left(D_M\left(\frac{T}{n}\right) - 1 \right) D'_N\left(\frac{T}{n}\right) \mathbb{E}[\zeta^3] \right|, \end{aligned}$$

where

$$\Gamma(n, M, N) \leq \frac{N(M+N)}{n} 8\pi^2 T^{\frac{1}{2}} \mathbb{E} \left[\sup_{[0,T]} \sigma^2(t) \right]^{\frac{3}{2}} + \frac{N}{\sqrt{2M+1}} 2\pi T^{\frac{1}{2}} \mathbb{E} \left[\sup_{[0,T]} \sigma^2(t) \right]^{\frac{3}{2}},$$

$$\Lambda(n, N) \leq \frac{N}{\sqrt{n}} 4\pi T^{\frac{1}{2}} \mathbb{E} \left[\sup_{[0,T]} \sigma^2(t) \right]^{\frac{3}{2}} + \frac{N^2}{n} 4\pi^2 (1 + T^{\frac{1}{2}}) \mathbb{E} \left[\sup_{[0,T]} \sigma^4(t) \right]^{\frac{1}{2}} \mathbb{E} \left[\sup_{[0,T]} \sigma^2(t) \right]^{\frac{1}{2}},$$

and,

$$\Psi(N) \leq \frac{1}{\sqrt{2N+1}} T \mathbb{E} \left[\sup_{[0,T]} \eta^2(t) \right]^{\frac{1}{2}}.$$

The mean squared error of the estimator (23) has the following bias-variance decomposition

$$\mathbb{E}[(\tilde{\eta}_{n,M,N} - \eta)^2] = \text{Var}(\tilde{\eta}_{n,M,N}) + \mathbb{E}[\tilde{\eta}_{n,M,N} - \eta]^2 + \text{Var}(\eta) - 2\text{Cov}(\tilde{\eta}_{n,M,N}, \eta). \quad (28)$$

This decomposition differs from the classical bias-variance decomposition which can be found in the parametric statistics literature because the quantity we aim to estimate, i.e. the integrated leverage effect η , is a random variable and not a constant parameter. We can show the following result.

Theorem 3.2. *We assume that (H1), (H2) and*

$$\frac{N^2}{M} \rightarrow 0 \quad \text{and} \quad \frac{MN}{n} \rightarrow 0 \quad (29)$$

hold true as $N, M, n \rightarrow \infty$ and $n \rightarrow \infty$, then

$$\mathbb{E}[(\tilde{\eta}_{n,M,N} - \eta)^2] \rightarrow \infty$$

The theorem above highlights the presence of a divergent element in (28). In the next section, we try to identify this element by means of numerical analysis and develop an optimal selection strategy for the cut-off parameters M and N .

The following corollary is important for Section 3.1.

Corollary 3.3. *We assume that Assumptions of Theorem 3.1 hold. Then, the addend (24) has expected value equal to zero.*

Proof. The term (24) can be decomposed as

$$\begin{aligned} & \sum_{i \neq j \neq k} D_M(t_i - t_j) D'_N(t_k - t_j) \delta_i \delta_j \delta_k \\ + & \sum_{i,j,k:i \neq j \neq k} D_M(t_i - t_j) D'_N(t_k - t_j) (\delta_i \delta_j \epsilon_k + \delta_j \delta_k \epsilon_i + \delta_k \delta_i \epsilon_j + \delta_i \epsilon_j \epsilon_k + \delta_j \epsilon_i \epsilon_k + \delta_k \epsilon_i \epsilon_j + \epsilon_i \epsilon_j \epsilon_k). \end{aligned}$$

Because of the results shown in the proof of Theorem 3.1, it follows directly that the expected value of (24) is equal to zero. ■

3.1 Optimal selection strategy for the cutting frequency parameters: a numerical study

We assume that the underlying efficient price process is described by two different models, i.e. the classical Heston model [21] and the generalized Heston model proposed in [35], and that the microstructure noise is modelled following Assumption (H2). Therefore, we will work on two data-sets.

We simulate second-by-second return and variance paths over a daily trading period of $T = 6$ hours, for a total of 100 trading days and $n = 21600$ observations per day.

The first data-set is simulated by the model

$$H : \begin{cases} dp(t) &= \sigma(t) dW_1(t) \\ d\sigma^2(t) &= \alpha(\beta - \sigma^2(t))dt + \nu\sigma(t) dW_2(t), \end{cases} \quad (30)$$

where W_1 and W_2 are correlated Brownian motions. The parameter values used in the simulations are $\alpha = 0.01, \beta = 0.2, \nu = 0.05$ and the correlation parameter is chosen as $\rho = -0.2$.

The second data-set is simulated by the model

$$GH : \begin{cases} dp(t) &= \sigma(t) dX(t) \\ dX(t) &= \rho(t) dW_1(t) + \sqrt{1 - \rho^2(t)} dW_2(t) \\ d\sigma^2(t) &= \alpha(\beta - \sigma^2(t))dt + \nu\sigma(t) dW_1(t), \end{cases} \quad (31)$$

and the infinitesimal variation of $\rho(t)$ is given by

$$d\rho(t) = ((2\xi - \eta) - \eta\rho(t))dt + \theta\sqrt{(1 + \rho(t))(1 - \rho(t))}dW_0,$$

where η, ξ and θ are positive constants and W_0 is a Brownian motion. The processes $W_0(t), W_1(t)$ and $W_2(t)$ are assumed to be independent. The parameter values used in the simulation are $\alpha = 0.01, \beta = 0.2, \nu = 0.05$ and $\xi = 0.02, \eta = 0.5, \theta = 0.5$, where the last three parameters are chosen in the range prescribed in [35] such that $\rho(t) \in [-1, 1]$. We set the initial values as $\sigma^2(0) = \beta, p(0) = \log(100)$ and $\rho(0) = -0.04$. The noise-to-signal ratio $std(\zeta)/std(r)$ is equal to 0.8, where r is the 1-second returns.

When processing simulated data, the natural approach in optimizing estimators concerning bandwidths or other parameters is to choose those values that minimize the finite sample mean squared error (MSE). Therefore, one possible choice is to select the cutting frequency parameters M and N by following this methodology. We present two types of MSE-based optimal strategies. The first one is simply based on minimizing the MSE of the FEL $\tilde{\eta}_{n,M,N}$ and the other one on the use of a variance corrected estimator of the FEL in the presence of microstructure noise. This strategy is presented below.

The term (24)

$$\Upsilon_{n,M,N} = \sum_{i,j,k: i \neq j \neq k} D_M(t_i - t_j) D'_N(t_k - t_j) \tilde{\delta}_i \tilde{\delta}_j \tilde{\delta}_k,$$

containing all the cross products of the noisy returns $\tilde{\delta}_i \tilde{\delta}_j \tilde{\delta}_k$ with $i \neq j \neq k$, has expected value equal to zero as shown in Corollary 3.3 and it is correlated to $\tilde{\eta}_{n,M,N}$.

We then define the estimator

$$\eta_{n,M,N}^* = \tilde{\eta}_{n,M,N} - b \Upsilon_{n,M,N} \tag{32}$$

which is an asymptotically unbiased estimator of the integrated leverage effect because of Theorem 3.1 and Corollary 3.3 and has

$$Var(\eta_{n,M,N}^*) = Var(\tilde{\eta}_{n,M,N}) - 2b Cov(\tilde{\eta}_{n,M,N}, \Upsilon_{n,M,N}) + b^2 Var(\Upsilon_{n,M,N}). \tag{33}$$

Hence, the estimator $\eta_{n,M,N}^*$ has smaller variance than the estimator $\tilde{\eta}_{n,M,N}$ if

$$b^2 Var(\Upsilon_{n,M,N}) < 2b Cov(\tilde{\eta}_{n,M,N}, \Upsilon_{n,M,N}).$$

The optimal coefficient b^* minimizing the variance of the estimator $\eta_{n,M,N}^*$ is given by

$$b_{M,N}^* = \frac{Cov(\tilde{\eta}_{n,M,N}, \Upsilon_{n,M,N})}{Var(\Upsilon_{n,M,N})}. \tag{34}$$

Substituting this values in (33) and simplifying, we find that

$$\frac{\text{Var}(\eta_{n,M,N}^*)}{\text{Var}(\tilde{\eta}_{n,M,N})} = (1 - \text{Corr}(\tilde{\eta}_{n,M,N}, \Upsilon_{n,M,N})^2),$$

which gives us the variance reduction obtained by using the estimator (32).

Remark 3.4. *Similar variance reduction appears when the classical control variate estimator is used, for example, to reduce the variance of the sample mean estimator, see ([20, Section 4.1]).*

Operatively, the variance corrected estimator (32) can be implemented by the following procedure:

Step 1: Given a sample of n observed returns and for all $M \in \{\text{range}\}$ and $N \in \{\text{range}\}$, let $\tilde{\eta}_{n,M,N}^1, \tilde{\eta}_{n,M,N}^2, \dots, \tilde{\eta}_{n,M,N}^d$ be d replications of the Fourier estimate of the integrated leverage in a Monte Carlo experiment. Along with $\tilde{\eta}_{n,M,N}^i$, on each replication we also calculate $\Upsilon_{n,M,N}^i$;

Step 2: let $M^*, N^* := \text{argmin VAR}(\Upsilon_{n,M,N})$ and let $\Upsilon^* := \Upsilon_{n,M^*,N^*}$;

Step 3: plug the selected correction Υ^* into equation (32)

$$\eta_{n,M,N}^* = \tilde{\eta}_{n,M,N} - b_{M,N}^* \Upsilon^*,$$

where

$$b_{M,N}^* = \frac{\text{COV}(\tilde{\eta}_{n,M,N}, \Upsilon^*)}{\text{VAR}(\Upsilon^*)}$$

and for each M and N , compute d replications $\eta_{n,M,N}^{i*}$ ($i = 1, \dots, d$) of the estimator¹;

Step 4: choose the cutting frequency parameters \hat{M} and \hat{N} which minimize the finite sample MSE of the corrected estimates $\eta_{n,M,N}^{i*}$ for $i = 1, \dots, d$.

The magnitude of the variance correction given by the estimator (32) is tuned by formula (34), where $\text{Var}(\Upsilon_{n,M,N})$ appears in the denominator. In our procedure, we first set the parameter (34) such to have the minimum possible denominator and to increase the effectiveness of the correction. Afterwards, in Step 4, we choose the optimal MSE-based cutting frequency parameters \hat{M} and \hat{N} . With these procedure, better results are empirically observed respect to simultaneously optimizing the parameters M and N appearing in (32).

Table 1 shows the MSE reduction obtained by using the estimator (32) versus the Fourier estimator $\tilde{\eta}_{n,M,N}$. The optimal parameter values \hat{M} and \hat{N} are obtained by following the MSE-based procedures described above. Since both estimators are only asymptotically unbiased and in the case of the Heston model the selected cutting frequency parameters \hat{M} and \hat{N} are rather

¹Note that COV and VAR denote the sample covariance and the sample variance, respectively.

	<i>H – model</i>				<i>GH – model</i>			
$\bar{\eta}$	-1.013673e-04				-4.603226e-05			
	MSE	BIAS	\hat{M}	\hat{N}	MSE	BIAS	\hat{M}	\hat{N}
$\tilde{\eta}_{n,M,N}$	2.40e-07	2.79e-05	887	1	1.70e-07	4.67e-06	2404	2
$\eta_{n,M,N}^*$	1.43e-07	4.63e-05	889	1	1.49e-07	4.76e-06	2638	1

Table 1: Finite sample performance of the FEL $\tilde{\eta}_{n,M,N}$ and of the estimator $\eta_{n,M,N}^*$. $\bar{\eta}$ represents the average real integrated leverage for each data set. The value of the MSE and BIAS in the table are computed w.r.t. the optimal parameters \hat{M} and \hat{N} .

small, the variance corrected estimator entails a slight increase of the bias, while for the generalized Heston model the bias remains almost the same. We notice that in both cases the optimal MSE-based \hat{M} turns out to be much smaller than the Nyquist frequency (i.e $\hat{M} \ll n/2$), whereas \hat{N} is very small, as prescribed by the asymptotic growth conditions in Theorem 2.2.

Let us now analyse the MSE and the sample variance (VAR) of the FEL in the presence of noise for the Heston and the generalized Heston model data sets as a function of M and N .

It is evident from Figure 1 that the sample variance of the estimator has an order of magnitude comparable with the one of the MSE. Moreover, by analysing the relative difference (MSE-VAR)/MSE for the FEL (23) and the estimator (32) as a function of M and N , we observe that this ratio is negligible for both estimators except for the lowest values of M and never exceeds 0.1 so that the difference MSE-VAR never exceeds 10% of the MSE.

We also find that the remaining terms in (28) are at least one order of magnitude smaller than the sample variance which is then the largest part of the MSE of the FEL in the presence of microstructure noise contamination in our simulated data set. The same conclusions apply when analysing the estimator (32). We conclude that minimizing the MSE of the Fourier estimators of the integrated leverage effect (23) or of the estimator (32), as a way to determine the optimal cutting frequencies parameters \hat{M} and \hat{N} , is equivalent to minimizing the sample variance of the estimators. Following this selection strategy, the cutting frequency parameters are not corresponding to a minimum value of the bias of the estimator. Then, the optimized estimator is affected by a non-negligible bias which is however very small. In our simulation, a significant digit after the comma is always obtained. Note that implementing this kind of selection strategy for the estimator (32) means changing the Step 4 of its implementation in accordance with the minimization of the sample variance. The results obtained by selecting optimal cutting frequencies parameters by minimizing the sample variance of the estimators (23) and (32) are displayed in Table 2. We highlight that the selected parameters M and N are the same as the ones selected by MSE minimization.

3.2 Benchmark analysis

We want now to analyse the performance of the FEL with respect to the estimator of the integrated leverage effect proposed by [29] in the presence of noise. The latter is based on pre-

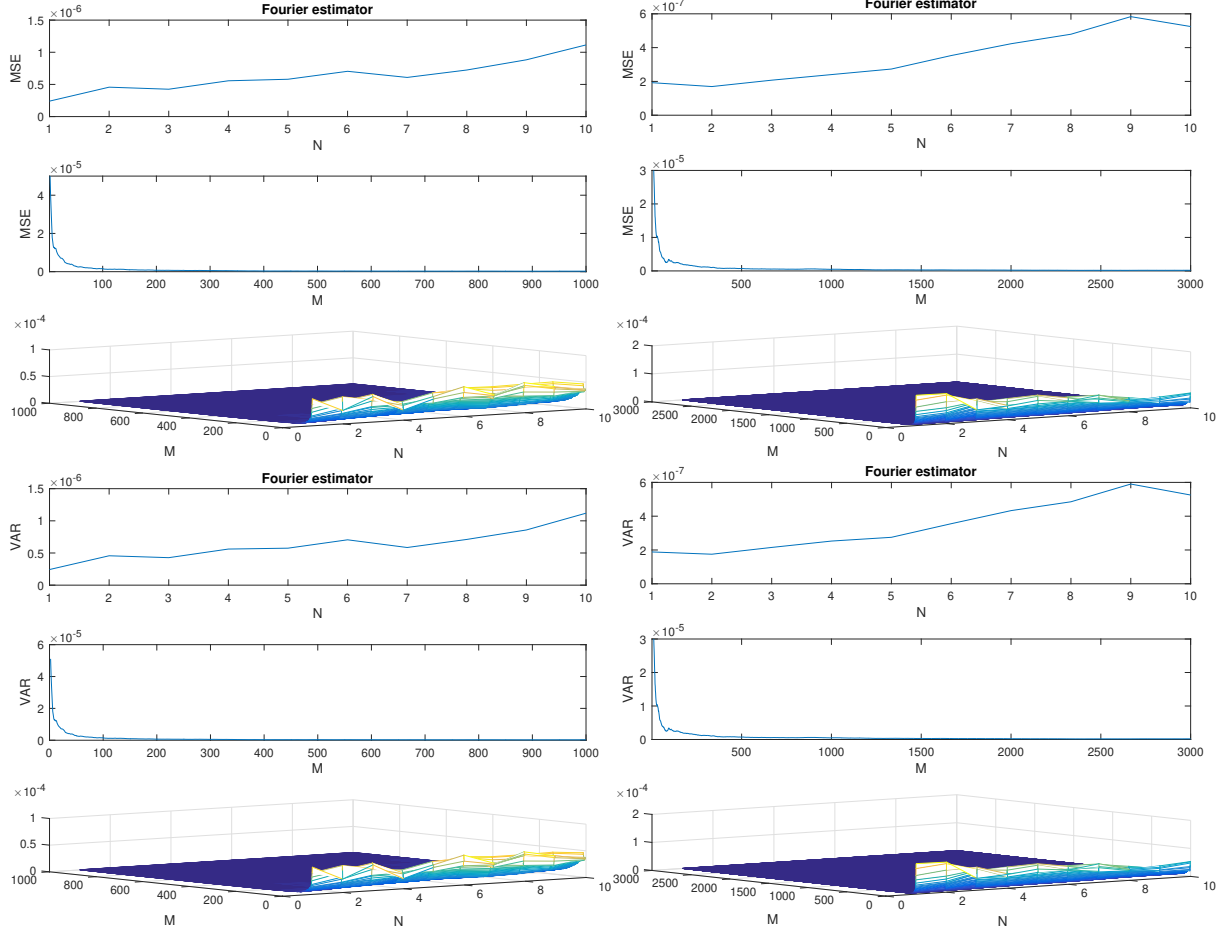


Figure 1: MSE and sample variance of the leverage estimate $\tilde{\eta}_{n,M,N}$ as a function of M and N under microstructure effects. Left panels: H model. Right panels: GH model.

averaging and blocking that allows to deal with the noise present in the data. Here two nested levels of blocks are required: the first one, of size M , defines the range of pre-averaging, and the second one, of size L is used for computing the realized covariance between returns and volatility increments. Our choice for the blocking parameters M and L is the following: we let M vary from 2 seconds to 300 seconds (i.e. 5 minute-block size). Then, up to rounding, for each value of M we define $n' = n/M$ and let $L = \lceil \sqrt{n'} \rceil$. Coherently with our previous approach, we then choose the optimal parameters by direct minimization of the MSE over the range of M 's. We call this estimator WM1.

In their paper, the authors provide a rule to choose the optimal values of M and L that minimize the asymptotic variance in the presence of microstructure effects. However, the implementation of this rule requires a preliminary estimate of the integrated volatility, of the integrated quarticity and the integrated sixth power of volatility, besides the estimation of the spot quarticity and of the diffusion coefficient $\gamma(t)$ in (1). In order to reduce possible sources of estimation errors, we compute the analytical values of these quantities from the model (30) by

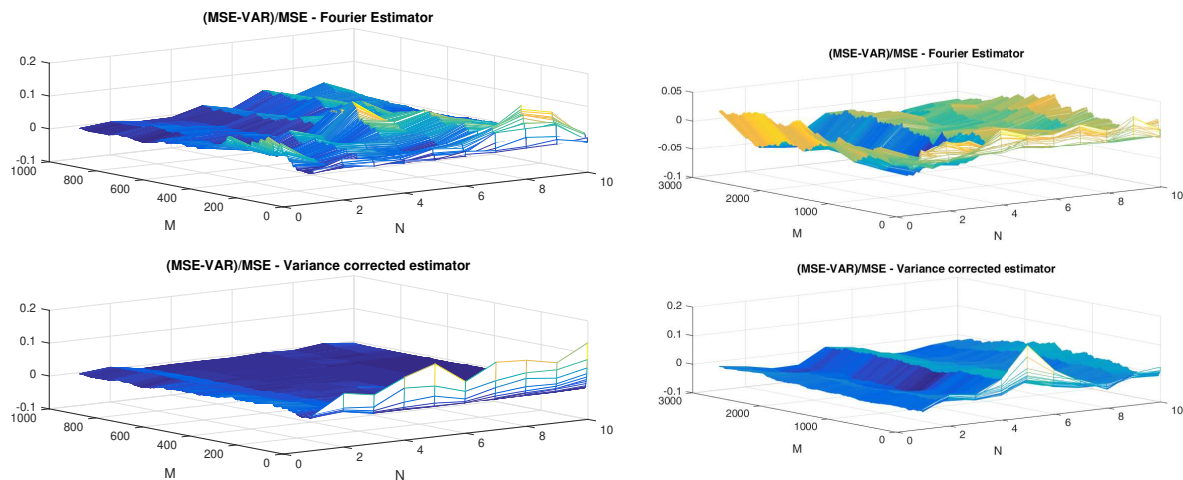


Figure 2: Relative difference between MSE and variance of the leverage estimate $\tilde{\eta}_{n,M,N}$ as a function of M and N under microstructure effects. Left panels: H model. Right panels: GH model.

	<i>H – model</i>				<i>GH – model</i>			
$\bar{\eta}$	-1.013673e-04				-4.603226e-05			
	VAR	λ	\hat{M}	\hat{N}	VAR	λ	\hat{M}	\hat{N}
$\tilde{\eta}_{n,M,N}$	2.43e-07		887	1	1.75e-07		2404	2
$\eta_{n,M,N}^*$	1.44e-07	0.59	889	1	1.51e-07	0.86	2638	1

Table 2: Finite sample performance of the FEL $\tilde{\eta}_{n,M,N}$ and of the estimator $\eta_{n,M,N}^*$. $\bar{\eta}$ represents the average real integrated leverage for each data set. The optimal parameters \hat{M} and \hat{N} are selected by minimization of the sample variance. The value of the VAR in the table is computed w.r.t. the optimal parameters \hat{M} and \hat{N} . The symbol λ denotes the variance reduction ratio $Var(\eta_{n,\hat{M},\hat{N}}^*)/Var(\tilde{\eta}_{n,\hat{M},\hat{N}})$.

Riemann integration rule. We call this estimator WM2. Our results are resumed in Table 3. We notice that the first procedure, which is completely unfeasible, provides a worse estimate than the Fourier methodology presented in Table 1 and 2 both in terms of bias and variance. On the other hand, the second procedure provides a very good estimate in terms of bias while the variance and MSE are nevertheless slightly larger than those obtainable by the Fourier approach. This does not come as a surprise, since the estimator proposed by Mykland and Wang contains a bias correction factor while in the Fourier case the unbiasedness is achieved only asymptotically. As a further evidence, in Figure 3 we can see that the estimate proposed by Wang and Mykland is largely dependent on the choice of the block size M and its MSE is increasing with this parameter, while the bias remains rather stable around zero.

Wang and Mykland, 2014	<i>H</i> – model				
Estimator	MSE	VAR	BIAS	<i>M</i>	<i>L</i>
WM1	3.90e-06	3.76e-06	-4.24e-04	4	73
WM2	3.09e-07	3.12e-07	-7.96e-06	2	2460

Table 3: Finite sample properties of the estimator by Wang and Mykland [29] under microstructure effects.

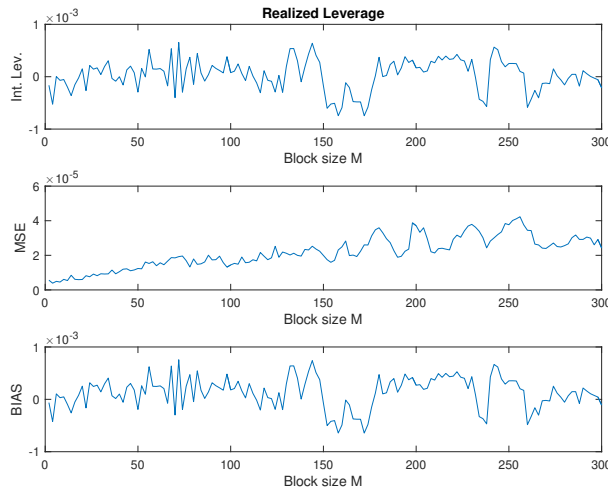


Figure 3: MSE-based integrated leverage estimate by Wang and Mykland [29] together with its MSE and BIAS as a function of the block size M .

3.3 Sensitivity analysis on the generalized Heston model

We examine the behaviour of the FEL in the presence of microstructure noise contamination depending on the choice of some parameters of the GH model. The process $\rho(t)$ in the GH model is a linear transformation of a Jacobi process which takes values in $[-1, 1]$. Moreover, $\rho(t)$ is mean reverting to $\zeta = (2\xi - \eta)/\eta$ at speed η . These kinds of processes are ideal diffusions to model stochastic correlation. Its properties are summarized in [35].

An interesting feature of this process is that it tends to a jump process with state-space $\{-1, 1\}$ and constant intensities if θ tends to infinity. Roughly speaking, when θ increases the process exhibits a jump-type behaviour while the smaller the parameter θ , the smoother are the sample paths. Therefore, the fluctuations of the process $\rho(t)$ can be amplified by increasing the parameter θ . Fig. 4 show the sensitivity of the FEL (23) and of the variance corrected estimator (32) with respect to the choice of θ in terms of MSE. All the other model parameters are taken as in Section 3.1 and the cutting frequencies are determined by minimization of the sample variance. As expected, the MSE of both estimators slightly deteriorates as the jump-type behaviour of the correlation process is emphasized.

We also examine the sensitivity of the FEL to the mean reversion parameter η . The effect is examined in Fig. 5, where the MSE is plotted as a function of ζ ranging in $[-1, 1]$ and of

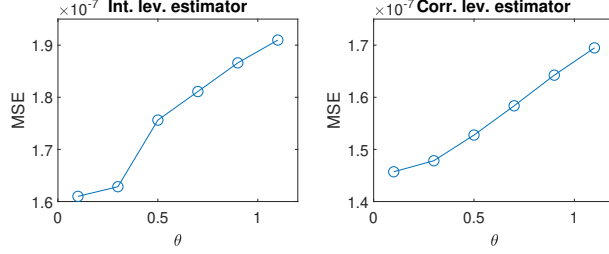


Figure 4: Sensitivity of the FEL $\tilde{\eta}_{n,M,N}$ and of the estimator $\eta_{n,M,N}^*$ with respect to the choice of θ in the presence of microstructure noise. Parameter values: $\alpha = 0.01, \beta = 0.2, \nu = 0.05$ and $\xi = 0.02, \eta = 0.5$.

the corresponding $\eta = 2\xi/(\zeta + 1)$. In this case, the variability of the MSE is small. Moreover, we highlight that the Fourier estimator is not much affected by the speed of mean reversion and performs slightly better when the speed of mean reversion is lower. This makes the Fourier methodology particularly suitable to be applied in a general setting where we can assume that the GH model is the data generating process.

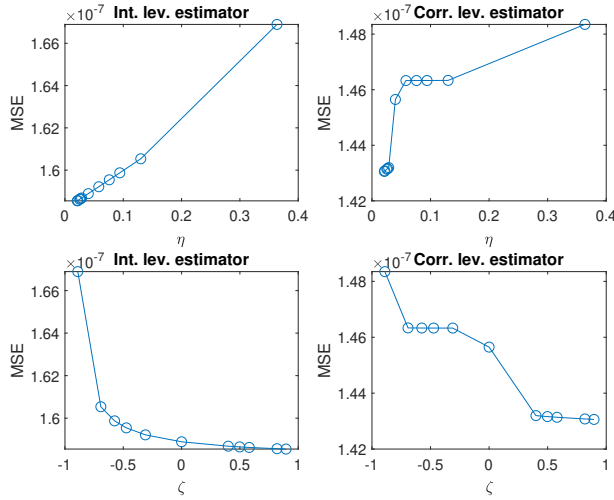


Figure 5: Sensitivity of the FEL $\tilde{\eta}_{n,M,N}$ and of the estimator $\eta_{n,M,N}^*$ with respect to the choice of η and $\zeta = (2\xi - \eta)/\eta$ in the presence of microstructure noise. Parameter values: $\alpha = 0.01, \beta = 0.2, \nu = 0.05$ and $\xi = 0.02, \theta = 0.5$.

4 Estimation of the stochastic leverage effect in the presence of microstructure noise

In the following, we denote by $\tilde{\sigma}_{n,M}^2$ and $\tilde{\gamma}_{n,M,N}^2$ the FEV and the FEVV in the presence of microstructure noise contamination, respectively. We can then obtain an estimation of (3) in the presence of microstructure noise contamination by using the FEL defined in (23) at the

numerator and $\tilde{\sigma}_{n,M}^2$ and $\tilde{\gamma}_{n,M,N}^2$ at the denominator

$$\tilde{R}_T = \frac{\tilde{\eta}_{n,M,N}}{\sqrt{\tilde{\sigma}_{n,M}^2 \tilde{\gamma}_{n,M,N}^2}}. \quad (35)$$

Similarly, we can also consider a second estimator of (3) by using the Fourier estimator $\eta_{n,M,N}^*$ defined in (32) at the numerator

$$R_T^* = \frac{\eta_{n,M,N}^*}{\sqrt{\tilde{\sigma}_{n,M}^2 \tilde{\gamma}_{n,M,N}^2}}. \quad (36)$$

The estimators (35) and (36) depend on the choice of some cutting frequencies that strongly affect the quality of the estimates.

For the FELs at the numerator, we follow the optimal selection strategy for the cutting frequencies M and N described in Section 3.1. If we have simulated data, we are going to generate a certain number of days of data and minimizing the sample variance of the FELs. On the other hand, if we are working in a real data framework, we need several days of observations (e.g. 100 days) to perform the parameter selection.

For the FEV $\tilde{\sigma}_{n,M}^2$ the cutting frequency is determined by minimizing the MSE estimate determined in [27, Theorem 3] on each day. Finally, for the FEVV $\tilde{\gamma}_{n,M,N}^2$ the frequencies M and N can be chosen in the range defined in [32, Remark 4.3].

In this section, we use simulated data and perform an estimation with real data in Section 5. We again simulate second-by-second return and variance paths over a daily trading period of $T = 6$ hours from the GH model (31) and choose the parameter values and the noise-to-signal ratio as in Section 3.1. The values of the cutting frequencies selected for the simulation are listed in Table 4, together with the MSE achieved by each estimator appearing in (35)-(36) and the average value over 100 days of the corresponding true (following the GH model) integrated leverage, integrated volatility and integrated volatility of volatility.

Process	Reference Value	MSE	M	N
$\tilde{\eta}_{n,M,N}$	-4.60e-05	1.70e-07	2404	2
$\eta_{n,M,N}^*$	-4.60e-05	1.49e-07	2638	1
$\tilde{\sigma}_{n,M}^2$	1.00e-02	2.38e-06	819	-
$\tilde{\gamma}_{n,M,N}^2$	2.51e-05	3.71e-07	146	3

Table 4: GH data set. MSE and cutting frequencies obtained for each estimator appearing in (35) and (36). The reference values corresponds to the average over 100 days of the corresponding true integrated values.

Figure 6 shows R_T estimated by using the FEL (23) and its variance corrected counterpart (32). The true R_T is plotted in red. In our simulation, both plots displayed in Figure 6 seem to be provide a good approximation of R_T .

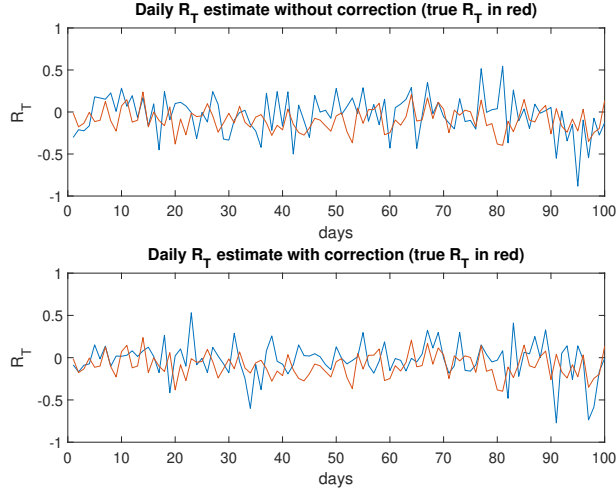


Figure 6: Upper panel: R_T estimated by \tilde{R}_T . Lower panel: R_T estimated by \tilde{R}_T^* . True R_T in red.

5 Empirical analysis

We analyse the leverage effect pattern in a tick data set by using the estimators of the stochastic leverage effect \tilde{R}_T and R_T^* as defined in (35) and (36), respectively.

We consider transaction data of the S&P500 futures recorded at the Chicago Mercantile Exchange (CME) for the period from 03 January 2007 to 31 December 2008 (502 days). During this period, the United States experienced the subprime mortgage crisis, a nationwide financial crisis that contributed to the U.S. recession of December 2007 till June 2009. It was triggered by a large decline in home prices after the collapse of a housing bubble during 2006. This induced a large banking crisis in 2007 and the financial crisis in 2008. In a nine-day period from October 1 to 9, 2008 the S&P500 lost 21.6% of its value. Table 5 describes the main features of our data set.

Year	N. trades	Variable	Mean	Std. Dev.	Min	Max
2007	566409	S&P 500 index	1484.84	44.30	1375.00	1586.50
		log-return	5.00e-6	1.81e-2	-1.64	2.33
2008	557982	S&P 500 index	1226.55	186.89	739.00	1480.20
		log-return	-9.03e-5	4.75e-2	-8.66	6.12

Table 5: Summary statistics for the sample of the traded CME S&P500 futures for the period from 03 January 2007 to 31 December 2008 (502 days).

Figure 7 shows the plot of the log-prices and returns for the raw transaction data. High-frequency returns are contaminated by transaction costs as bid-and-ask bounce effects, leading to biases in the variance measures. Figure 8 shows the autocorrelation function for the log-returns. Raw data exhibit a strongly significant positive first-order autocorrelation and higher-order autocorrelations remain significant up to lag 8 in 2007 and up to lag 15 in 2008.

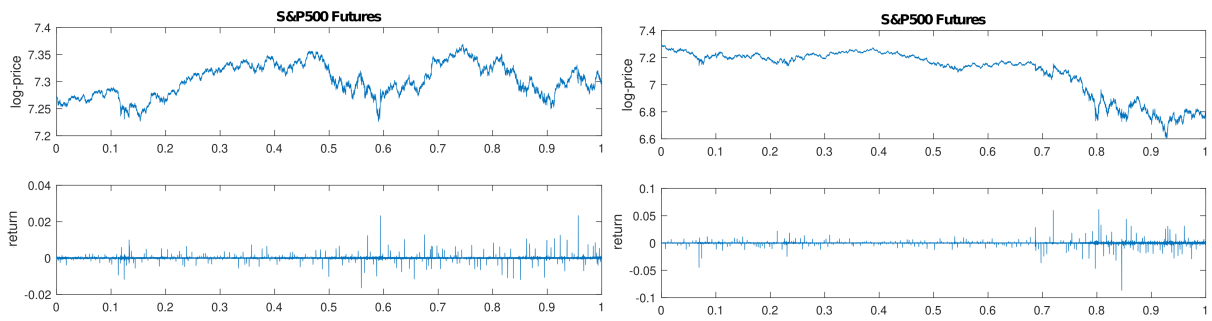


Figure 7: Log-prices and returns plots for S&P500 futures in the years 2007 (left panels) and 2008 (right panels).

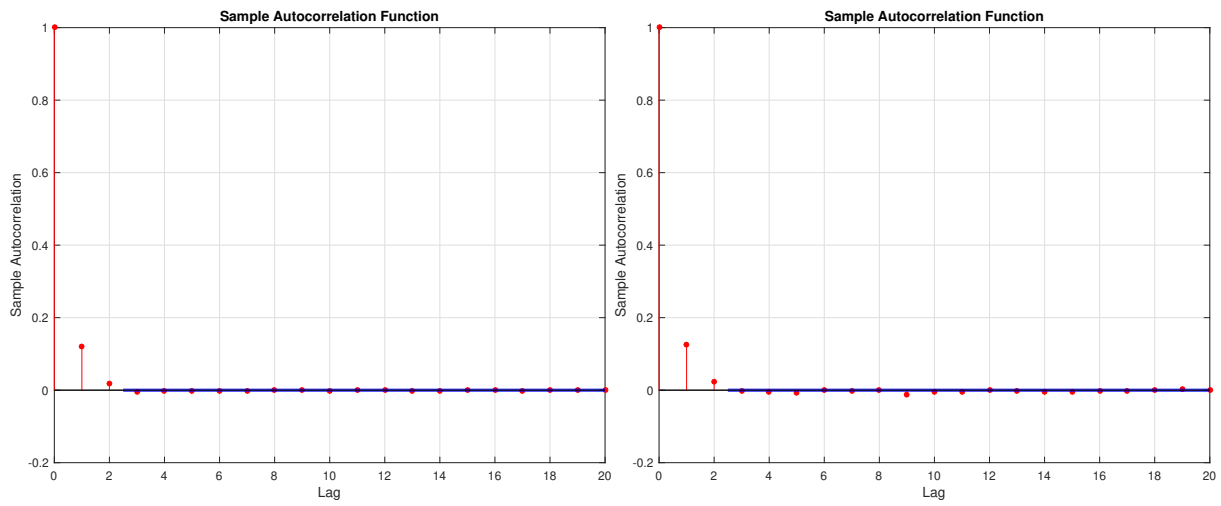


Figure 8: Autocorrelation function for S&P500 futures in the years 2007 (left panel) and 2008 (right panel).

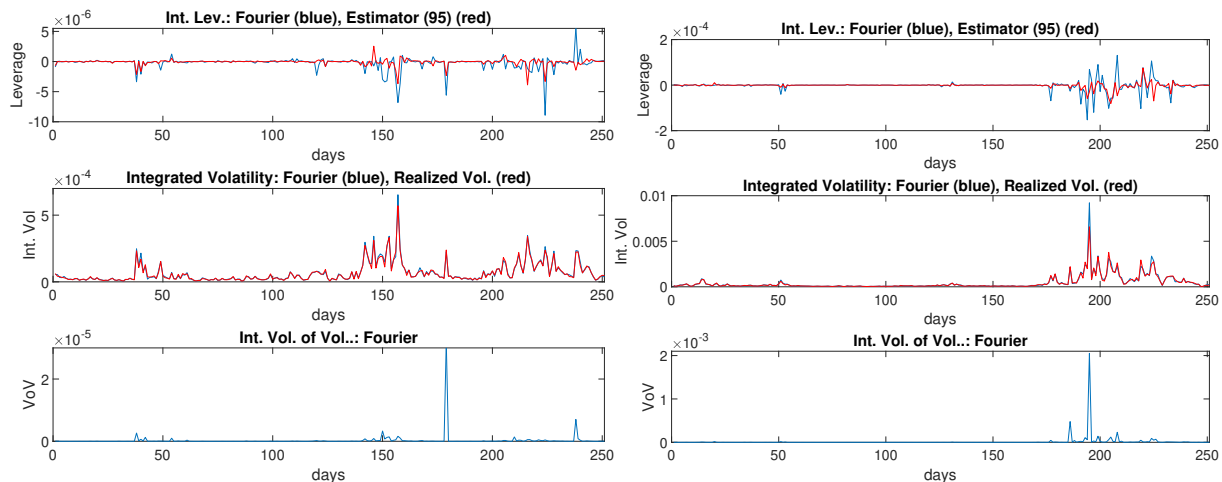


Figure 9: Upper panel: FEL (17) (blue) and estimator (32) (red) . Middle panel: FEV (blue) and the realized volatility estimator (red) in the years 2007 (left panel) and 2008 (right panel). Lower panel: FEVV (blue) in the years 2007 (left panel) and 2008 (right panel).

We then perform an analysis of the stochastic leverage effect using the estimators \tilde{R}_T and R_T^* . First, we plot the daily values of the factors appearing in the estimator \tilde{R}_T and R_T^* . The upper panels of Figure 9 show the daily FEL (23) and its variance corrected version (32) in 2007 and 2008. The middle panels show the FEV together with the 5-minute sparse sampled realized volatility estimator (which we consider as a benchmark of our estimates) and the lower panels show the FEVV in 2007 and 2008. The values on the vertical axes in the plots on the left (2007) and on the right (2008) are different from one year to another due to the different magnitudes of the estimates. The year 2008 displays the largest values (both negative and positive) of all the metrics, coherently with the occurrence of the financial crisis. During 2007 the integrated leverage is rather small and mostly negative. All the estimations are almost flat during 2008 up to September 16 (day 177 in our sample), when the integrated leverage exhibits the first large negative spike. The second slightly negative spike is on September 29 (day 186), which corresponds to the beginning of the financial crisis. Our finding highlights the presence of persistent positive and negative integrated leverage effect, especially in periods of financial turmoil. We notice that both the FEL (23) and the corrected estimator (32) catch the same positive and negative spikes of the integrated leverage but the variability of the estimator (32) is mitigated.

When estimating the leverage effect, a larger variability in the estimates can be observed if compared to other quantities such as volatility or quarticity. According to the analysis of Section 4, for both estimators the cutting frequency parameters M and N are chosen such to minimize the sample variance over the whole one year sample. Their optimal values are listed in Table 6, along with the sample variance achieved by the FEL (23) and its variance corrected counterpart (32). Due to the presence of microstructure effects, the optimal cutting frequency M turns out to be much smaller than the Nyquist frequency (i.e. $M \ll n/2 = 2460$).

S&P500 futures	2007					2008				
	Estimate	VAR	λ	\hat{M}	\hat{N}	Estimate	VAR	λ	\hat{M}	\hat{N}
$\tilde{\eta}_{n,M,N}$	-2.44e-07	1.20e-12		363	1	-2.01e-06	5.94e-10		281	3
$\eta_{n,M,N}^*$	-9.23e-08	3.02e-13	0.25	143	1	-1.76e-06	1.51e-10	0.25	285	3

Table 6: The FEL, its variance corrected counterpart (32) and their sample variance computed w.r.t. the cutting frequencies \hat{M} and \hat{N} . The symbol λ denotes the variance reduction ratio $Var(\eta_{n,\hat{M},\hat{N}}^*)/Var(\tilde{\eta}_{n,\hat{M},\hat{N}})$. The optimal cutting frequency parameters are obtained by minimization of the sample variance over each year. The estimate in the first column corresponds to the average over all the year of the daily estimates.

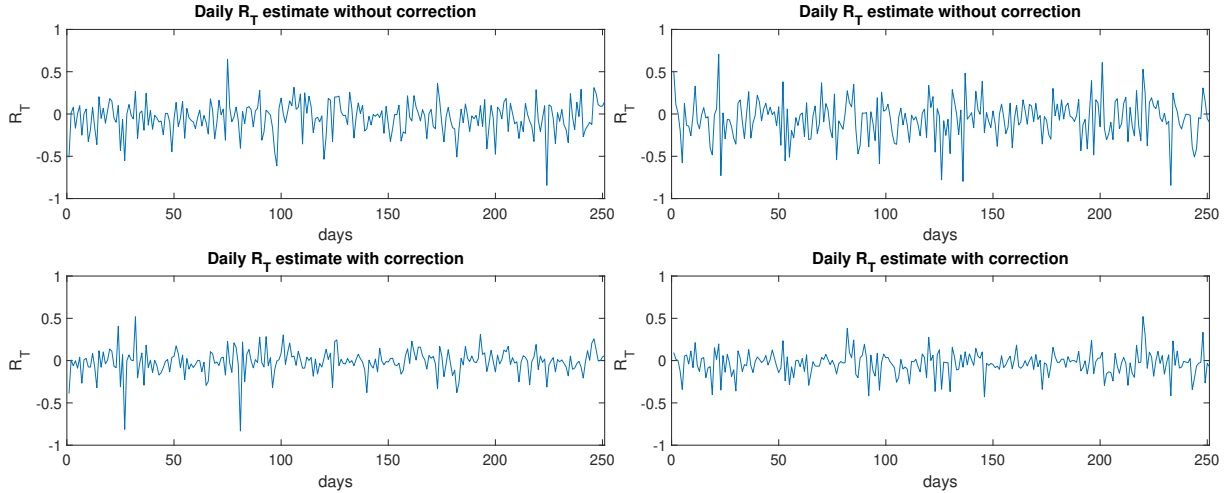


Figure 10: R_T estimated by the estimator (35) (upper panels) and by the estimator (36) (lower panels) in the years 2007 (left panels) and 2008 (right panels).

We remark that the Fourier estimator makes use of all the n observed prices because it reconstructs the signal in the frequency domain and it filters out microstructure effects by a suitable choice of M and N instead of reducing the sampling frequency.

We conclude this section by showing the plot of the estimator \hat{R}_T when using estimator (35) and (36). The plots do not show evident differences between the years 2007 and 2008. This is exactly how it should be. In fact, big fluctuations of the returns and of its respective volatilities do not affect the fundamental value of R_T due to its definition. In fact, we expect to see a similar behaviour of R_T in both years (remember we assume that the data generating process is the same for both the 2007 and 2008 data sets) which gives a *fundamental measure* of the asymmetry between returns and volatilities observed across the years.

Appendix: Proofs

Proof of Theorem 2.2: Throughout the proof we indicate with $\phi_n(s) := \sup_{k=0, \dots, n} \{t_k : t_k \leq s\}$. Moreover, we use the following integral notation for the discrete Fourier coefficients of the returns (15)

$$c_n(s; dp) = \frac{1}{T} \int_0^T e^{-i\frac{2\pi}{T}s\phi_n(u)} dp(u).$$

In the proof, C will denote a positive constant, not necessarily the same at different occurrences.

Applying the product rule to the term $c_n(s; dp)c_n(l-s; dp)$ and using notations (9) and (10), we obtain the following error decomposition.

$$\eta_{n,M,N} - \eta = \eta_{n,N}^1 - \eta + \eta_{n,M,N}^2 \quad (37)$$

$$= \underbrace{\frac{T^2}{2N+1} \sum_{|l| \leq N} il \frac{2\pi}{T} \frac{1}{T} \int_0^T e^{-i\frac{2\pi}{T}l\phi_n(t)} \sigma^2(t) dt \frac{1}{T} \int_0^T e^{i\frac{2\pi}{T}l\phi_n(u)} dp(u) - \int_0^T \eta(t) dt}_{\eta_{n,N}^1} \quad (38)$$

$$+ \underbrace{\frac{T^2}{2N+1} \sum_{|l| \leq N} il \frac{2\pi}{T} \left(\frac{1}{T} \int_0^T \int_0^t e^{-i\frac{2\pi}{T}l\phi_n(u)} D_M(\phi_n(t) - \phi_n(u)) dp(u) dp(t) \right)}_{\eta_{n,M,N}^2}$$

$$+ \underbrace{\frac{1}{T} \int_0^T e^{-i\frac{2\pi}{T}l\phi_n(t)} \int_0^t D_M(\phi_n(t) - \phi_n(u)) dp(u) dp(t) \frac{1}{T} \int_0^T e^{i\frac{2\pi}{T}l\phi_n(u)} dp(u)}_{\eta_{n,M,N}^2}, \quad (39)$$

where the variable $t \in (0, T]$. By using the Cauchy-Schwartz inequality we have that

$$\begin{aligned} \mathbb{E}[|\eta_{n,M,N}^2|] &\leq \frac{T^2}{2N+1} \sum_{|l| \leq N} |l| \frac{2\pi}{T} \mathbb{E} \left[\left| \frac{1}{T} \int_0^T \int_0^t e^{-i\frac{2\pi}{T}l\phi_n(u)} D_M(\phi_n(t) - \phi_n(u)) dp(u) dp(t) \right|^2 \right]^{\frac{1}{2}} \\ &\quad + \frac{1}{T} \int_0^T e^{-i\frac{2\pi}{T}l\phi_n(t)} \int_0^t D_M(\phi_n(t) - \phi_n(u)) dp(u) dp(t) \left| \frac{1}{T} \int_0^T e^{i\frac{2\pi}{T}l\phi_n(u)} dp(u) \right|^2 \right]^{\frac{1}{2}}. \end{aligned}$$

For each $|l| \leq N$, the L_2 -norm of the Fourier coefficients of the returns

$$\mathbb{E} \left[\left| \int_0^T e^{i\frac{2\pi}{T}l\phi_n(u)} dp(u) \right|^2 \right] \leq C,$$

under Assumption (H1). On the other hand,

$$\begin{aligned} & \mathbb{E} \left[\left| \frac{1}{T} \int_0^T \int_0^t e^{-i\frac{2\pi}{T}l\phi_n(u)} D_M(\phi_n(t) - \phi_n(u)) dp(u) dp(t) \right. \right. \\ & \quad \left. \left. + \frac{1}{T} \int_0^T e^{-i\frac{2\pi}{T}l\phi_n(t)} \int_0^t D_M(\phi_n(t) - \phi_n(u)) dp(u) dp(t) \right|^2 \right] \\ & \leq C \mathbb{E} \left[\left| \frac{1}{T} \int_0^T \int_0^t e^{-i\frac{2\pi}{T}l\phi_n(u)} D_M(\phi_n(t) - \phi_n(u)) dp(u) dp(t) \right|^2 \right] \end{aligned} \quad (40)$$

$$+ C \mathbb{E} \left[\left| \frac{1}{T} \int_0^T e^{-i\frac{2\pi}{T}l\phi_n(t)} \int_0^t D_M(\phi_n(t) - \phi_n(u)) dp(u) dp(t) \right|^2 \right]. \quad (41)$$

The addends (40) and (41) have the same order of magnitude in L_2 -norm. We then show only the estimation of the term (40). The latter is less than or equal to

$$\begin{aligned} & \underbrace{C \mathbb{E} \left[\left| \frac{1}{T} \int_0^T \int_0^t (e^{-i\frac{2\pi}{T}l\phi_n(u)} - e^{-i\frac{2\pi}{T}lu}) \frac{1}{2M+1} \sum_{|s| \leq M} e^{-i\frac{2\pi}{T}s(\phi_n(t) - \phi_n(u))} dp(u) dp(t) \right|^2 \right]}_{(T_1)} \\ & + C \mathbb{E} \left[\left| \frac{1}{T} \int_0^T \int_0^t e^{-i\frac{2\pi}{T}l\phi_n(u)} \frac{1}{2M+1} \sum_{|s| \leq M} (e^{-i\frac{2\pi}{T}s(\phi_n(t) - \phi_n(u))} - e^{-i\frac{2\pi}{T}s(t-u)}) dp(u) dp(t) \right|^2 \right] \\ & \quad \underbrace{\hspace{15em}}_{(T_2)} \\ & \quad + C \mathbb{E} \left[\left| \frac{1}{T} \int_0^T \int_0^t e^{-i\frac{2\pi}{T}lu} D_M(t-u) dp(u) dp(t) \right|^2 \right]. \end{aligned} \quad (T_3)$$

The term (T_1) , after applying the Itô isometry, is less than or equal to

$$\begin{aligned} & C \mathbb{E} \left[\int_0^T \left| \int_0^t (e^{-i\frac{2\pi}{T}l\phi_n(u)} - e^{-i\frac{2\pi}{T}lu}) \frac{1}{2M+1} \sum_{|s| \leq M} e^{-i\frac{2\pi}{T}s(\phi_n(t) - \phi_n(u))} dp(u) \right|^2 \sigma^2(t) dt \right] \\ & \quad \underbrace{\hspace{15em}}_{(T_{11})} \\ & + C \mathbb{E} \left[\int_{[0,T]^2} \left(\int_0^t (e^{-i\frac{2\pi}{T}l\phi_n(u)} - e^{-i\frac{2\pi}{T}lu}) \frac{1}{2M+1} \sum_{|s| \leq M} e^{-i\frac{2\pi}{T}s(\phi_n(t) - \phi_n(u))} dp(u) \right) \right. \\ & \quad \left. \left(\int_0^z (e^{i\frac{2\pi}{T}l\phi_n(v)} - e^{i\frac{2\pi}{T}lv}) \frac{1}{2M+1} \sum_{|s| \leq M} e^{i\frac{2\pi}{T}s(\phi_n(z) - \phi_n(v))} dp(v) \right) a(z) a(t) dz dt \right] \\ & \quad \underbrace{\hspace{15em}}_{(T_{12})} \\ & \leq C \mathbb{E} \left[\int_0^T \int_0^t (|l| \frac{2\pi}{T} |\phi_n(t) - t| + l^2 \frac{4\pi^2}{T^2} o(|\phi_n(t) - t|^2))^2 du dt \right] \end{aligned}$$

$$\begin{aligned}
& + C\mathbb{E} \left[\int_0^T \int_{[0,t]^2} (|l| \frac{2\pi}{T} |\phi_n(t)-t| + l^2 \frac{4\pi^2}{T^2} o(|\phi_n(t)-t|^2)) (|l| \frac{2\pi}{T} |\phi_n(s)-s| + l^2 \frac{4\pi^2}{T^2} o(|\phi_n(s)-s|^2)) dv ds dt \right] \\
& + C(N^2\tau(n) + o(1))\mathbb{E} \left[\int_{[0,T]^2} \left(\int_0^t \frac{1}{2M+1} \sum_{|s|\leq M} e^{-i\frac{2\pi}{T}s(\phi_n(t)-\phi_n(u))} dp(u) \right. \right. \\
& \quad \left. \left. \int_0^z \frac{1}{2M+1} \sum_{|s|\leq M} e^{i\frac{2\pi}{T}s(\phi_n(z)-\phi_n(v))} dp(v) \right) a(z) a(t) dz dt \right].
\end{aligned}$$

To obtain the last inequality, we apply several times Taylor's formula, Assumption (H1) and the Hölder and Cauchy-Schwarz inequalities. Note that the first two addends from the right hand side correspond to the estimation of the term (T_{11}) whereas the third addend estimates from above (T_{12}) . Thus,

$$\mathbb{E}[(T_1)] \leq CN^2\tau^2(n) + o(1).$$

Analogously, we can show that

$$\mathbb{E}[(T_2)] \leq CM^2\tau^2(n) + o(1).$$

It remains to analyse the last addend of (40).

$$\begin{aligned}
& \mathbb{E}[(T_3)] \leq C\mathbb{E} \left[\int_0^T \left| \int_0^t e^{-i\frac{2\pi}{T}lu} D_M(t-u) dp(u) \right|^2 \sigma^2(t) dt \right] \\
& + \left[\int_{[0,T]^2} \left(\int_0^t e^{-i\frac{2\pi}{T}lu} D_M(t-u) dp(u) \int_0^z e^{i\frac{2\pi}{T}lz} D_M(z-v) dp(v) \right) a(t) a(z) dt dz \right].
\end{aligned}$$

Using iteratively the Hölder and the Cauchy-Schwarz inequalities, we obtain the term above is less than or equal to

$$\begin{aligned}
& \leq C\mathbb{E} \left[\int_0^T \int_0^t D_M^2(t-u) \sigma^2(u) du dt \right] + C\mathbb{E} \left[\int_0^T \left(\int_0^t |D_M(t-u)|^{p'} a(u) du \right)^{\frac{2}{p'}} dt \right] \\
& + C\mathbb{E} \left[\int_{[0,T]^2} \left(\int_0^t D_M^2(t-u) du \right) dt dz \right]^{\frac{1}{2}} \mathbb{E} \left[\int_{[0,T]^2} \left(\int_0^z D_M^2(z-v) dv \right) dt dz \right]^{\frac{1}{2}} \\
& + C\mathbb{E} \left[\int_{[0,T]^2} \left(\int_0^t |D_M(t-u)|^{p'} du \right)^{\frac{2}{p'}} dt dz \right]^{\frac{1}{2}} \mathbb{E} \left[\int_{[0,T]^2} \left(\int_0^z D_M^2(z-v) dv \right) dt dz \right]^{\frac{1}{2}} \\
& + C\mathbb{E} \left[\int_{[0,T]^2} \left(\int_0^t D_M^2(t-u) du \right) dt dz \right]^{\frac{1}{2}} \mathbb{E} \left[\int_{[0,T]^2} \left(\int_0^z |D_M(z-v)|^{p'} dv \right)^{\frac{2}{p'}} dt dz \right]^{\frac{1}{2}} \\
& + C\mathbb{E} \left[\int_{[0,T]^2} \left(\int_0^t |D_M(t-u)|^{p'} du \right)^{\frac{2}{p'}} dt dz \right]^{\frac{1}{2}} \mathbb{E} \left[\int_{[0,T]^2} \left(\int_0^z |D_M(z-v)|^{p'} dv \right)^{\frac{2}{p'}} dt dz \right]^{\frac{1}{2}},
\end{aligned}$$

for $p' \in (1, 2)$. By Proposition 2.1,

$$\mathbb{E}[(T_3)] \leq \frac{C}{2M+1} + \frac{C}{(2M+1)^{\frac{2}{p'}}} + \frac{C}{(2M+1)^{\frac{2+p'}{2p'}}}.$$

Thus

$$E[|\eta_{n,M,N}^2|] \leq C \frac{N}{\sqrt{M+1}} + CN^2\tau(n) + CNM\tau(n) + o(1),$$

which converges to zero under Assumption (18). We now show that the term (38) converges to zero in L_1 -norm.

$$\begin{aligned} & \mathbb{E}[|\eta_{n,N}^1 - \eta|] \\ &= \mathbb{E}\left[\left|\frac{1}{2N+1} \sum_{|l| \leq N} il \frac{2\pi}{T} \sum_{i=0}^{n-1} \sum_{j=0}^{n-1} e^{i\frac{2\pi}{T}l(t_i-t_j)} \int_{t_j}^{t_{j+1}} \sigma^2(t) dt \int_{t_i}^{t_{i+1}} dp(u) - \int_0^T \eta(t) dt\right|\right] \\ &= \mathbb{E}\left[\left|\frac{1}{2N+1} \sum_{|l| \leq N} il \frac{2\pi}{T} \int_0^T \int_0^T (e^{i\frac{2\pi}{T}l(\phi_n(t)-\phi_n(u))} - e^{i\frac{2\pi}{T}l(t-u)}) \sigma^2(u) du a(t) dt\right|\right] \end{aligned} \quad (42)$$

$$+ \mathbb{E}\left[\left|\frac{1}{2N+1} \sum_{|l| \leq N} il \frac{2\pi}{T} \int_0^T \int_0^T (e^{i\frac{2\pi}{T}l(\phi_n(t)-\phi_n(u))} - e^{i\frac{2\pi}{T}l(t-u)}) \sigma^2(u) du \sigma(t) dW(t)\right|\right] \quad (43)$$

$$+ \mathbb{E}\left[\left|\frac{1}{2N+1} \sum_{|l| \leq N} il \frac{2\pi}{T} \int_0^T e^{-i\frac{2\pi}{T}lu} \sigma^2(u) du \int_0^T e^{i\frac{2\pi}{T}lt} dp(t) - \int_0^T \eta(t) dt\right|\right]. \quad (44)$$

By using Taylor's formula, the term (42) is less than or equal to

$$\begin{aligned} & C \frac{1}{2N+1} \sum_{|l| \leq N} |l| \frac{2\pi}{T} \mathbb{E}\left[\int_0^T \int_0^T e^{-i\frac{2\pi}{T}l(t-u)} \left(\frac{2\pi}{T} |l| |\phi_n(t) - t - \phi_n(u) + u| \right. \right. \\ & \quad \left. \left. + l^2 \frac{4\pi^2}{T^2} o(|\phi_n(t) - t - \phi_n(u) + u|^2) du dt\right) \right] \\ & \leq CN^2\tau(n) + o(1). \end{aligned}$$

Analogously, term (43) is less than or equal to $CN^2\tau(n)$. Let us analyse the term (44). By using formula (11)

$$\begin{aligned} & \mathbb{E}\left[\left|\frac{1}{2N+1} \sum_{|l| \leq N} il \frac{2\pi}{T} \int_0^T e^{-i\frac{2\pi}{T}lu} \sigma^2(u) du \int_0^T e^{i\frac{2\pi}{T}lt} dp(t) - \int_0^T \eta(t) dt\right|\right] \\ &= \mathbb{E}\left[\left|\frac{T^2}{2N+1} \sum_{|l| \leq N} il \frac{2\pi}{T} c(l; \sigma^2) c(-l; dp) - \int_0^T \eta(t) dt\right|\right] \end{aligned}$$

$$= \mathbb{E} \left[\left| \frac{1}{2N+1} \sum_{|l| \leq N} \left(c(l; d\sigma^2) - \frac{1}{T} \int_0^T d\sigma^2(u) \right) c(-l; dp) - \int_0^T \eta(t) dt \right| \right].$$

We use now the product rule and obtain

$$\begin{aligned} & \mathbb{E} \left[\left| \int_0^T \int_0^t D_N(t-u) dp(u) d\sigma^2(t) + \int_0^T \int_0^t D_N(t-u) d\sigma^2(u) dp(t) \right. \right. \\ & \quad \left. \left. - \int_0^T \int_0^t D_N(u) dp(u) d\sigma^2(t) - \int_0^T \int_0^t D_N(t) d\sigma^2(u) dp(t) - \int_0^T D_N(u) \eta(u) du \right| \right]. \end{aligned}$$

Let us analyse the first double integral $M_{1,N}(T)$

$$\begin{aligned} \mathbb{E} \left[\left| \int_0^T \int_0^t D_N(t-u) dp(u) d\sigma^2(s) \right| \right] &= \mathbb{E} \left[\left| \int_0^T \int_0^t D_N(t-u) \sigma(u) dW(u) \gamma(s) dZ(s) \right. \right. \\ & \quad \left. \left. + \int_0^T \int_0^t D_N(t-u) \sigma(u) dW(u) b(s) ds + \int_0^T \int_0^t D_N(t-u) a(u) d(u) \gamma(s) dZ(s) \right. \right. \\ & \quad \left. \left. + \int_0^T \int_0^t D_N(t-u) a(u) du b(s) ds \right| \right] \end{aligned}$$

The first two summands of the decomposition above have a L_1 -norm of order $O(N^{-\frac{1}{2}})$ and the third and the fourth ones are of order $O(N^{-\frac{1}{p}})$, where $p \in (1, 2)$. These estimations are performed by means of the use of Proposition 2.1, the Hölder and Cauchy-Schwarz inequality. Analogous calculations follow for the terms $M_{1,N}(T)$, $M_{2,N}(T)$, $M_{3,N}(T)$, $M_{4,N}(T)$.

By Proposition 2.1, we have

$$\mathbb{E} [|M_{5,N}(2\pi)|] \leq C \mathbb{E} \left[\sup_{t \in [0, T]} |\eta(t)| \right] \left(\int_0^T |D_N(u)|^p du \right)^{\frac{1}{p}} \leq \frac{C}{N^{\frac{1}{p}}}.$$

Choosing $p \in (1, 2)$ we obtain that the term $M_{5,N}(2\pi)$ converges to zero in L_1 -norm as $N \rightarrow \infty$. Thus,

$$\begin{aligned} \mathbb{E} \left[\left| \frac{4\pi^2}{2N+1} \sum_{|l| \leq N} i l c(l; \nu) c(-l; dp) - \int_0^{2\pi} \eta(t) dt \right| \right] \\ \leq \frac{C}{\sqrt{N}} + \frac{C}{N^{\frac{1}{p}}} \end{aligned}$$

Therefore, under Assumption (18), it follows the consistency of the estimator $\eta_{n,M,N}$. ■

Proof of Theorem 3.1. We first analyse the Bias due to the noise components.

Because of Assumption (H2), it holds

$$\begin{aligned}\mathbb{E}[\epsilon_i \epsilon_j \epsilon_k] &= 0 \text{ if } i \neq j \neq k \\ \mathbb{E}[\epsilon_i^2 \epsilon_j] &= \begin{cases} 0 & \text{if } |i-j| \neq 1, \\ -\mathbb{E}[\zeta^3] & \text{if } j = i+1, \\ \mathbb{E}[\zeta^3] & \text{if } j = i-1, \end{cases}\end{aligned}$$

and

$$\begin{aligned}\mathbb{E}[\eta_{n,M,N}^\epsilon] &= \sum_{i=0}^{n-1} \sum_{j=0}^{n-1} D'_N(t_i - t_j) \mathbb{E}[\epsilon_j^2 \epsilon_i] + \sum_{i=0}^{n-1} \sum_{j=0}^{n-1} D_M(t_i - t_j) D'_N(t_i - t_j) \mathbb{E}[\epsilon_i^2 \epsilon_j] \\ &= \sum_{i=0}^{n-2} D'_N(t_{i+1} - t_i) \mathbb{E}[\epsilon_i^2 \epsilon_{i+1}] + \sum_{i=1}^{n-1} D'_N(t_{i-1} - t_i) \mathbb{E}[\epsilon_i^2 \epsilon_{i-1}] \\ &+ \sum_{i=0}^{n-2} D_M(t_{i+1} - t_i) D'_N(t_{i+1} - t_i) \mathbb{E}[\epsilon_{i+1}^2 \epsilon_i] + \sum_{i=1}^{n-1} D_M(t_{i-1} - t_i) D'_N(t_{i-1} - t_i) \mathbb{E}[\epsilon_{i-1}^2 \epsilon_i] \\ &= (n-1) D'_N\left(\frac{T}{n}\right) \mathbb{E}[\epsilon_i^2 \epsilon_{i+1}] + (n-1) D'_N\left(-\frac{T}{n}\right) \mathbb{E}[\epsilon_i^2 \epsilon_{i-1}] \\ &+ (n-1) D_M\left(\frac{T}{n}\right) D'_N\left(\frac{T}{n}\right) \mathbb{E}[\epsilon_{i+1}^2 \epsilon_i] + D_M\left(\frac{T}{n}\right) D'_N\left(-\frac{T}{n}\right) \mathbb{E}[\epsilon_{i-1}^2 \epsilon_i] \\ &= 2(n-1) D'_N\left(\frac{T}{n}\right) (D_M\left(\frac{T}{n}\right) - 1) \mathbb{E}[\zeta^3].\end{aligned}$$

By using Taylor's formula, it follows that $D'_N\left(\frac{T}{n}\right) \sim O\left(\frac{N^2}{n}\right)$ and $D_M\left(\frac{T}{n}\right) \sim 1 - O\left(\frac{M^2}{n^2}\right)$. Thus, under the Assumption (27), $|\mathbb{E}[\eta_{n,M,N}^\epsilon]|$ converges to zero as $N, M, n \rightarrow \infty$.

The expected value of the term (25) is equal to

$$\sum_{i,j,k: i \neq j \neq k} D_M(t_i - t_j) D'_N(t_k - t_j) \mathbb{E}[\delta_i \delta_j \delta_k] = 0,$$

because $\mathbb{E}[\delta_i \delta_j \delta_k] = 0$.

The expected value of the term involving the components (26) equals

$$\begin{aligned}& \mathbb{E}\left[\frac{1}{2N+1} \sum_{|l| \leq N} il \frac{2\pi}{T} \frac{1}{2M+1} \sum_{|s| \leq M} \sum_{i=0}^{n-1} \sum_{j=0}^{n-1} e^{i \frac{2\pi}{T} (l-s)(t_i - t_j)} \delta_i^2 \delta_j\right. \\ & \quad \left. + \frac{1}{2N+1} \sum_{|l| \leq N} il \frac{2\pi}{T} \sum_{i=0}^{n-1} \sum_{j=0}^{n-1} e^{i \frac{2\pi}{T} l(t_i - t_j)} \delta_i \delta_j^2 - \int_0^T \eta(t) dt\right] \\ &= \mathbb{E}\left[\frac{1}{2N+1} \sum_{|l| \leq N} il \frac{2\pi}{T} \frac{1}{2M+1} \sum_{|s| \leq M} \sum_{i=0}^{n-1} \sum_{j=0}^{n-1} e^{i \frac{2\pi}{T} (l-s)(t_i - t_j)} \int_{t_i}^{t_{i+1}} \sigma^2(u) du \int_{t_j}^{t_{j+1}} dp(t)\right] \\ & \quad (A_1)\end{aligned}$$

$$+\mathbb{E}\left[\frac{1}{2N+1}\sum_{|l|\leq N}il\frac{2\pi}{T}\frac{1}{2M+1}\sum_{|s|\leq M}\sum_{i=0}^{n-1}\sum_{j=0}^{n-1}e^{i\frac{2\pi}{T}(l-s)(t_i-t_j)}\int_{t_i}^{t_{i+1}}\int_{t_i}^t dp(u)dp(t)\int_{t_j}^{t_{j+1}} dp(t)\right]$$

(A₂)

$$+\mathbb{E}\left[\frac{1}{2N+1}\sum_{|l|\leq N}il\frac{2\pi}{T}\sum_{i=0}^{n-1}\sum_{j=0}^{n-1}e^{i\frac{2\pi}{T}l(t_i-t_j)}\int_{t_j}^{t_{j+1}}\int_{t_j}^t dp(u)dp(t)\int_{t_i}^{t_{i+1}} dp(t)\right]$$

(A₃)

$$+\mathbb{E}\left[\frac{1}{2N+1}\sum_{|l|\leq N}il\frac{2\pi}{T}\sum_{i=0}^{n-1}\sum_{j=0}^{n-1}e^{i\frac{2\pi}{T}l(t_i-t_j)}\int_{t_j}^{t_{j+1}}\sigma^2(u)du\int_{t_i}^{t_{i+1}} dp(t)-\int_0^T\eta(t)dt\right].$$

(A₄)

The term (A₁) can be further decomposed in

$$\mathbb{E}\left[\frac{1}{2N+1}\sum_{|l|\leq N}il\frac{2\pi}{T}\frac{1}{2M+1}\sum_{|s|\leq M}\sum_{i=1}^{n-1}\sum_{j=0}^{i-1}e^{i\frac{2\pi}{T}(l-s)(t_i-t_j)}\int_{t_i}^{t_{i+1}}\sigma^2(u)du\int_{t_j}^{t_{j+1}} dp(t)\right]$$

(A₁^{*})

$$+\mathbb{E}\left[\frac{1}{2N+1}\sum_{|l|\leq N}il\frac{2\pi}{T}\frac{1}{2M+1}\sum_{|s|\leq M}\sum_{j=1}^{n-1}\sum_{i=0}^{j-1}e^{i\frac{2\pi}{T}(l-s)(t_i-t_j)}\int_{t_i}^{t_{i+1}}\sigma^2(u)du\int_{t_j}^{t_{j+1}} dp(t)\right].$$

By applying the tower property with respect to the sigma-algebra \mathcal{F}_{i+1} , the second summand is zero because of the martingale property of the Itô integrals. Thus, the term (A₁) is just equal to the term (A₁^{*}). We call $|(A_1^*)| = \Gamma(n, M, N)$.

$$\begin{aligned}\Gamma(n, M, N) &= \left|\mathbb{E}\left[\frac{1}{2N+1}\sum_{|l|\leq N}il\frac{2\pi}{T}\int_0^T\int_0^te^{i\frac{2\pi}{T}l(\phi_n(t)-\phi_n(u))}\frac{1}{2M+1}\right.\right. \\ &\quad \left.\left.\sum_{|s|\leq M}e^{-i\frac{2\pi}{T}s(\phi_n(t)-\phi_n(u))}dp(u)\sigma^2(t)dt\right]\right| \\ &= \left|\mathbb{E}\left[\frac{1}{2N+1}\sum_{|l|\leq N}il\frac{2\pi}{T}\int_0^T\int_0^te^{i\frac{2\pi}{T}l(\phi_n(t)-\phi_n(u))}\frac{1}{2M+1}\right.\right. \\ &\quad \left.\left.\sum_{|s|\leq M}(e^{-i\frac{2\pi}{T}s(\phi_n(t)-\phi_n(u))}-e^{-i\frac{2\pi}{T}s(t-u)})dp(u)\sigma^2(t)dt\right]\right| \\ &\quad + \left|\mathbb{E}\left[\frac{1}{2N+1}\sum_{|l|\leq N}il\frac{2\pi}{T}\int_0^T\int_0^t(e^{-i\frac{2\pi}{T}l(\phi_n(t)-\phi_n(u))}-e^{-i\frac{2\pi}{T}l(t-u)})\right.\right. \\ &\quad \left.\left.\frac{1}{2M+1}\sum_{|s|\leq M}e^{-i\frac{2\pi}{T}s(t-u)}dp(u)\sigma^2(t)dt\right]\right| \\ &\quad + \left|\mathbb{E}\left[\frac{1}{2N+1}\sum_{|l|\leq N}il\frac{2\pi}{T}\int_0^T\int_0^te^{-i\frac{2\pi}{T}l(t-u)}D_M(t-u)dp(u)\sigma^2(t)dt\right]\right|.\end{aligned}$$

The third summand is less than or equal to

$$\begin{aligned} & \mathbb{E} \left[\frac{1}{2N+1} \sum_{|l| \leq N} |l| \frac{2\pi}{T} \left| \int_0^T \int_0^t e^{-i\frac{2\pi}{T}l(t-u)} D_M(t-u) dp(u) \sigma^2(t) dt \right| \right] \\ & \leq \frac{1}{2N+1} \sum_{|l| \leq N} |l| \frac{2\pi}{T} \mathbb{E} \left[\sup_{[0,T]} \sigma^2(t) \right]^{\frac{3}{2}} T \mathbb{E} \left[\int_0^T D_M^2(u) du \right]^{\frac{1}{2}} \leq 2\pi N \mathbb{E} \left[\sup_{[0,T]} \sigma^2(t) \right]^{\frac{3}{2}} \left(\frac{T}{2M+1} \right)^{\frac{1}{2}} \end{aligned}$$

by using the Cauchy Schwartz and Hölder inequality, the Itô isometry and the properties of the rescaled Dirichlet kernel.

By means of the Taylor's formula, we obtain estimations for the first and second summand of $\Gamma(n, M, N)$ as follows

$$\begin{aligned} & \left| \mathbb{E} \left[\frac{1}{2N+1} \sum_{|l| \leq N} il \frac{2\pi}{T} \int_0^T \int_0^t e^{i\frac{2\pi}{T}l(\phi_n(t)-\phi_n(u))} \frac{1}{2M+1} \right. \right. \\ & \quad \left. \left. \sum_{|s| \leq M} (e^{-i\frac{2\pi}{T}s(\phi_n(t)-\phi_n(u))} - e^{-i\frac{2\pi}{T}s(t-u)}) dp(u) \sigma^2(t) dt \right] \right| \\ & \leq \mathbb{E} \left[\left| \frac{1}{2N+1} \sum_{|l| \leq N} il \frac{2\pi}{T} \int_0^T \int_0^t e^{i\frac{2\pi}{T}l(\phi_n(t)-\phi_n(u))} \frac{1}{2M+1} \right. \right. \\ & \quad \left. \left. \sum_{|s| \leq M} e^{-i\frac{2\pi}{T}s(t-u)} (s \frac{2\pi}{T} (t-u - \phi_n(t) + \phi_n(u)) + o(1)) dp(u) \sigma^2(t) dt \right| \right] \\ & \leq \frac{1}{2N+1} \sum_{|l| \leq N} |l| \frac{2\pi}{T} \frac{1}{2M+1} \sum_{|s| \leq M} \mathbb{E} \left[\sup_{[0,T]} \sigma^2(t) \right] \\ & \int_0^T \mathbb{E} \left[\left| \int_0^t e^{i\frac{2\pi}{T}l(\phi_n(t)-\phi_n(u))} e^{-i\frac{2\pi}{T}s(t-u)} (s \frac{2\pi}{T} (t-u - \phi_n(t) + \phi_n(u)) + o(1)) dp(u) \right| \right] dt \\ & \leq \frac{1}{2N+1} \sum_{|l| \leq N} |l| \frac{2\pi}{T} \frac{1}{2M+1} \sum_{|s| \leq M} \mathbb{E} \left[\sup_{[0,T]} \sigma^2(t) \right] \\ & \quad \int_0^T \mathbb{E} \left[\int_0^t (s^2 \frac{4\pi^2}{T^2} (t-u - \phi_n(t) + \phi_n(u))^2 + o(1)) \sigma^2(u) du \right]^{\frac{1}{2}} dt \\ & \leq \frac{1}{2N+1} \sum_{|l| \leq N} |l| \frac{2\pi}{T} \frac{1}{2M+1} \sum_{|s| \leq M} \mathbb{E} \left[\sup_{[0,T]} \sigma^2(t) \right]^{\frac{3}{2}} \int_0^T \left(\int_0^t s^2 4 \frac{4\pi^2}{n^2} + o(1) du \right)^{\frac{1}{2}} dt \\ & \leq \frac{MN}{n} 8\pi^2 T^{\frac{1}{2}} \mathbb{E} \left[\sup_{[0,T]} \sigma^2(t) \right]^{\frac{3}{2}} + o(1), \end{aligned}$$

and

$$\left| \mathbb{E} \left[\frac{1}{2N+1} \sum_{|l| \leq N} il \frac{2\pi}{T} \int_0^T \int_0^t (e^{-i\frac{2\pi}{T}l(\phi_n(t)-\phi_n(u))} - e^{-i\frac{2\pi}{T}l(t-u)}) \right. \right.$$

$$\begin{aligned}
& \left| \frac{1}{2M+1} \sum_{|s| \leq M} e^{-i\frac{2\pi}{T}s(t-u)} dp(u) \sigma^2(t) dt \right| \\
\leq & \frac{1}{2N+1} \sum_{|l| \leq N} |l| \frac{2\pi}{T} \frac{1}{2M+1} \sum_{|s| \leq M} \mathbb{E} \left[\sup_{[0,T]} \sigma^2(t) \right]^{\frac{3}{2}} \int_0^T \left(\int_0^t (l^2 \frac{4\pi^2}{T^2} (\phi_n(t) - \phi_n(u) - t+u)^2 + o(1)) du \right)^{\frac{1}{2}} dt \\
& \leq \frac{N^2}{n} 8\pi^2 T^{\frac{1}{2}} \mathbb{E} \left[\sup_{[0,T]} \sigma^2(t) \right]^{\frac{3}{2}} + o(1).
\end{aligned}$$

Let us now further decompose the term (A_4) in

$$(A_4) = \mathbb{E} \left[\frac{1}{2N+1} \sum_{|l| \leq N} il \frac{2\pi}{T} \int_0^T e^{-il\frac{2\pi}{T}\phi_n(u)} \sigma^2(u) du \left(\int_0^T e^{il\frac{2\pi}{T}\phi_n(t)} - e^{il\frac{2\pi}{T}t} dp(t) \right) \right] \tag{A4.1}$$

$$+ \mathbb{E} \left[\frac{1}{2N+1} \sum_{|l| \leq N} il \frac{2\pi}{T} \int_0^T e^{il\frac{2\pi}{T}\phi_n(t)} dp(t) \left(\int_0^T e^{-il\frac{2\pi}{T}\phi_n(u)} - e^{-il\frac{2\pi}{T}u} \sigma^2(u) du \right) \right] \tag{A4.2}$$

$$+ \mathbb{E} \left[\frac{1}{2N+1} \sum_{|l| \leq N} il \frac{2\pi}{T} \int_0^T e^{-il\frac{2\pi}{T}u} \sigma^2(u) du \int_0^T e^{il\frac{2\pi}{T}t} dp(t) - \int_0^T \eta(t) dt \right]. \tag{A4.3}$$

We call $\Lambda(n, N) = |(A_2)| + |(A_3)| + |(A_{4.1})| + |(A_{4.2})|$.

Let us first discuss the terms (A_2) and (A_3) . For $i \neq j$, the terms

$$\frac{1}{2N+1} \sum_{|l| \leq N} il \frac{2\pi}{T} \frac{1}{2M+1} \sum_{|s| \leq M} \sum_{i \neq j} e^{i\frac{2\pi}{T}(l-s)(t_i-t_j)} \mathbb{E} \left[\int_{t_i}^{t_{i+1}} \int_{t_i}^t dp(u) dp(t) \int_{t_j}^{t_{j+1}} dp(t) \right]$$

and

$$\frac{1}{2N+1} \sum_{|l| \leq N} il \frac{2\pi}{T} \sum_{i \neq j} e^{i\frac{2\pi}{T}l(t_i-t_j)} \mathbb{E} \left[\int_{t_j}^{t_{j+1}} \int_{t_j}^t dp(u) dp(t) \int_{t_i}^{t_{i+1}} dp(t) \right]$$

are zero because the Itô integrals appearing in the expectations are defined on non overlapping intervals. For $i = j$, let us evaluate the terms $|(A_2)|$ and $|(A_3)|$. In this instance, (A_2) and (A_3) are both equal and

$$\begin{aligned}
& \left| \mathbb{E} \left[\frac{1}{2N+1} \sum_{|l| \leq N} il \frac{2\pi}{T} \sum_{i=0}^{n-1} \int_{t_i}^{t_{i+1}} \int_{t_i}^t dp(u) dp(t) \int_{t_i}^{t_{i+1}} dp(t) \right] \right| \\
& \leq \left| \frac{1}{2N+1} \sum_{|l| \leq N} il \frac{2\pi}{T} \sum_{i=0}^{n-1} \mathbb{E} \left[\int_{t_i}^{t_{i+1}} \int_{t_i}^t dp(u) \sigma^2(t) dt \right] \right|
\end{aligned}$$

$$\begin{aligned}
&\leq \frac{1}{2N+1} \sum_{|l| \leq N} |l| \frac{2\pi}{T} \sum_{i=0}^{n-1} \mathbb{E} \left[\left| \int_{t_i}^{t_{i+1}} \int_{t_i}^t dp(u) \sigma^2(t) dt \right| \right] \\
&\leq N \frac{2\pi}{T} \sum_{i=0}^{n-1} \mathbb{E} \left[\sup_{[0,T]} \sigma^2(t) \right]^{\frac{3}{2}} (t_{i+1} - t_i)^{\frac{3}{2}} \\
&\leq N \frac{2\pi}{T} \left(\frac{T}{n} \right)^{\frac{3}{2}} n \mathbb{E} \left[\sup_{[0,T]} \sigma^2(t) \right]^{\frac{3}{2}} = \frac{N}{\sqrt{n}} 2\pi T^{\frac{1}{2}} \mathbb{E} \left[\sup_{[0,T]} \sigma^2(t) \right]^{\frac{3}{2}},
\end{aligned}$$

by using the Itô isometry and the Hölder inequality. Moreover, because of the Cauchy-Schwartz inequality, $|(A_{4.1})|$ is less than or equal to

$$\begin{aligned}
&\frac{1}{2N+1} \sum_{|l| \leq N} |l| \frac{2\pi}{T} \mathbb{E} \left[\left| \int_0^T e^{-il \frac{2\pi}{T} \phi_n(u)} \sigma^2(u) du \right|^2 \right]^{\frac{1}{2}} \mathbb{E} \left[\left| \int_0^T e^{il \frac{2\pi}{T} \phi_n(t)} - e^{il \frac{2\pi}{T} \phi_n(t)} dp(t) \right|^2 \right]^{\frac{1}{2}} \\
&\leq \frac{1}{2N+1} \sum_{|l| \leq N} |l| \frac{2\pi}{T} \mathbb{E} \left[\int_0^T \sigma^4(u) du \right]^{\frac{1}{2}} T^{\frac{1}{2}} \mathbb{E} \left[\int_0^T (l \frac{2\pi}{T} \frac{T}{n} + o(1))^2 \sigma^2(t) dt \right]^{\frac{1}{2}} \\
&\quad \frac{1}{2N+1} \sum_{|l| \leq N} |l| \frac{2\pi}{T} \mathbb{E} \left[\sup_{t \in [0,T]} \sigma^4(t) \right]^{\frac{1}{2}} \mathbb{E} \left[\sup_{t \in [0,T]} \sigma^2(t) \right]^{\frac{1}{2}} T \frac{N}{n} 2\pi + o(1) \\
&\leq \frac{N^2}{n} 4\pi^2 \mathbb{E} \left[\sup_{t \in [0,T]} \sigma^4(t) \right]^{\frac{1}{2}} \mathbb{E} \left[\sup_{t \in [0,T]} \sigma^2(t) \right]^{\frac{1}{2}} + o(1),
\end{aligned}$$

by applying Taylor's Formula and the Cauchy-Schwartz inequality. Analogously, it can be shown that $|(A_{4.2})|$ is less than or equal to

$$\frac{N^2}{n} 4\pi^2 T^{\frac{1}{2}} \mathbb{E} \left[\sup_{t \in [0,T]} \sigma^4(t) \right]^{\frac{1}{2}} \mathbb{E} \left[\sup_{t \in [0,T]} \sigma^2(t) \right]^{\frac{1}{2}} + o(1).$$

It remains to evaluate the term $|(A_{4.3})|$ that we call $\Psi(N)$. By formula (11), $|(A_{4.3})|$ can be expressed as

$$\begin{aligned}
&\left| \mathbb{E} \left[\int_0^T \int_0^t D_N(t-u) dp(u) d\sigma^2(t) + \int_0^T \int_0^t D_N(t-u) d\sigma^2(u) dp(t) \right. \right. \\
&\quad \left. \left. - \int_0^T \int_0^t D_N(u) dp(u) d\sigma^2(t) - \int_0^T \int_0^t D_N(t) d\sigma^2(u) dp(t) - \int_0^T D_N(u) \eta(u) du \right] \right|.
\end{aligned}$$

The Itô integrals have zero mean and the terms above are simply equal to

$$\left| \mathbb{E} \left[- \int_0^T D_N(u) \eta(u) du \right] \right| \leq \mathbb{E} \left[\int_0^T D_N^2(u) du \int_0^T \eta(u)^2 du \right]^{\frac{1}{2}}$$

after applying the Cauchy-Schwartz inequality. Thus,

$$\Psi(N) \leq \frac{T}{\sqrt{2N+1}} \mathbb{E}[\sup_{t \in [0, T]} \eta(t)^2]^{\frac{1}{2}}.$$

The terms $\Gamma(n, M, N)$, $\Lambda(n, N)$ and $\Omega(N)$ converge to zero under Assumption (27) which concludes the proof. \blacksquare

Proof of Theorem 3.2. We have that

$$\begin{aligned} \mathbb{E}[(\tilde{\eta}_{n, M, N} - \eta)^2] &= \mathbb{E}\left[\left(\sum_{i, j, k: i \neq j \neq k} D_M(t_i - t_j) D'_N(t_k - t_j) \tilde{\delta}_i \tilde{\delta}_j \tilde{\delta}_k \right. \right. \\ &\quad \left. \left. + \sum_{i, j: i \neq j} D_M(t_i - t_j) D'_N(t_i - t_j) \tilde{\delta}_i^2 \tilde{\delta}_j + \sum_{i, j} D'_N(t_i - t_j) \tilde{\delta}_i \tilde{\delta}_j^2 - \eta\right)^2\right] \end{aligned} \quad (45)$$

which is in turn equal to

$$\begin{aligned} &\mathbb{E}\left[\left((\eta_{n, M, N} - \eta) \right. \right. \\ &\quad \left. \left. + \left(\sum_{i, j, k: i \neq j \neq k} D_M(t_i - t_j) D'_N(t_k - t_j) (\delta_i \delta_j \epsilon_k + \delta_j \delta_k \epsilon_i + \delta_k \delta_i \epsilon_j + \delta_i \epsilon_j \epsilon_k + \delta_j \epsilon_i \epsilon_k + \delta_k \epsilon_i \epsilon_j + \epsilon_i \epsilon_j \epsilon_k)\right) \right. \right. \\ &\quad \left. \left. + \left(\sum_{i, j: i \neq j} D_M(t_i - t_j) D'_N(t_i - t_j) (\delta_i \epsilon_j + \epsilon_i^2 \delta_j + \epsilon_j^2 \epsilon_i + 2\delta_j \delta_i \epsilon_i + 2\delta_i \epsilon_j \epsilon_i)\right) \right. \right. \\ &\quad \left. \left. + \left(\sum_{i, j} D'_N(t_i - t_j) (\delta_j \epsilon_i + \epsilon_j^2 \delta_i + \epsilon_j^2 \epsilon_i + 2\delta_j \delta_i \epsilon_j + 2\delta_j \epsilon_i \epsilon_j)\right)\right)^2\right]. \end{aligned}$$

The term $\mathbb{E}[(\eta_{n, M, N} - \eta)^2]$ corresponds to the mean squared error of the estimator (17) in the absence of microstructure noise contamination and converges to zero as n, M, N tend to infinity. The error decomposition (37) and the proof of Theorem 2.2 highlight that the term $\eta_{n, N}^1$ is in L_2 -norm bigger than $(\eta_{n, M, N}^2 - \eta)$. Then, to prove our claim, it is enough to analyse the convergence to zero of

$$\mathbb{E}[(\eta_{n, N}^1 - \eta)^2]. \quad (46)$$

Following Remark 2.3, we have that (46) is equal to

$$\begin{aligned} &\mathbb{E}\left[\left(\frac{1}{2N+1} \sum_{|l| \leq N} il \frac{2\pi}{T} \int_0^T \int_0^T (e^{i\frac{2\pi}{T}l(\phi_n(t) - \phi_n(u))} - e^{i\frac{2\pi}{T}l(t-u)}) \sigma^2(u) du \sigma(t) dW(t) \right. \right. \\ &\quad \left. \left. + \int_0^T \int_0^t D_N(t-u) dp(u) d\sigma^2(t) + \int_0^T \int_0^t D_N(t-u) d\sigma^2(t) dp(u) \right. \right. \\ &\quad \left. \left. - \int_0^T \int_0^t D_N(u) dp(u) d\sigma^2(t) - \int_0^T \int_0^t D_N(u) d\sigma^2(t) dp(u) - \int_0^T D_N(u) \eta(u) du\right)^2\right] \end{aligned}$$

$$\leq 2\mathbb{E}\left[\left(\frac{1}{2N+1}\sum_{|l|\leq N}il\frac{2\pi}{T}\int_0^T\int_0^T(e^{i\frac{2\pi}{T}l(\phi_n(t)-\phi_n(u))}-e^{i\frac{2\pi}{T}l(t-u)})\sigma^2(u)du\sigma(t)dW(t)\right)^2\right] \quad (47)$$

$$+ 8\mathbb{E}\left[\left(\int_0^T\int_0^tD_N(t-u)dp(u)d\sigma^2(t)\right)^2\right]+8\mathbb{E}\left[\left(\int_0^T\int_0^tD_N(t-u)dp(u)d\sigma^2(t)\right)^2\right] \quad (48)$$

$$+ 8\mathbb{E}\left[\left(\int_0^TD_N(u)\eta(u)du\right)^2\right]+8\mathbb{E}\left[\left(\int_0^TD_N(u)\eta(u)du\right)^2\right] \quad (49)$$

$$\leq \frac{128\pi^2}{T^2}\frac{N^4}{n^2}\mathbb{E}\left[\sup_{t\in[0,T]}\sigma^2(t)\right]\mathbb{E}\left[\sup_{t\in[0,T]}\sigma^4(t)\right] \quad (50)$$

$$+ 16\frac{T^2}{2N+1}\mathbb{E}\left[\sup_{t\in[0,T]}\sigma^2(t)\right]\mathbb{E}\left[\sup_{t\in[0,T]}\gamma^2(t)\right] \quad (51)$$

$$+ 16\frac{T}{2N+1}\mathbb{E}\left[\sup_{t\in[0,T]}\eta(t)^2\right], \quad (52)$$

where (50), (51), (52) correspond to the estimation of the summands (47), (48), (49), respectively. Thus, (46) converges to zero as $n, N \rightarrow \infty$ and so does the mean squared error of the estimator (17). However, whenever a noise component appears in the decomposition (45), the related terms diverge to infinity as n, M, N goes to infinity. As exemplary calculation, we will show that

$$\mathbb{E}\left[\left(\sum_{i,j}D'_N(t_i-t_j)(\delta_j\epsilon_i+\epsilon_j^2\delta_i+\epsilon_j^2\epsilon_i+2\delta_j\delta_i\epsilon_j+2\delta_j\epsilon_i\epsilon_j)\right)^2\right] \quad (53)$$

diverges as $n, N \rightarrow \infty$ and is greater than $O(n^2N)$. In order to handle the other terms in (45), the strategies of computation addressed below have to be used. Ultimately, this leads to show that the remaining terms in (45) are greater than $O(NM^2+\frac{n^2N}{M})$.

We have that

$$\begin{aligned} & \mathbb{E}\left[\left(\sum_{i,j}D'_N(t_i-t_j)\delta_j\epsilon_i+\epsilon_j^2\delta_i+\epsilon_j^2\epsilon_i+2\delta_j\delta_i\epsilon_j+2\delta_j\epsilon_i\epsilon_j\right)^2\right] \\ &= \sum_{i,j}(D'_N(t_i-t_j))^2\mathbb{E}[(\delta_j\epsilon_i+\epsilon_j^2\delta_i+\epsilon_j^2\epsilon_i+2\delta_j\delta_i\epsilon_j+2\delta_j\epsilon_i\epsilon_j)^2] \end{aligned} \quad (54)$$

$$\begin{aligned} & + \sum_{i,j,i',j':i\neq i',j\neq j'}D'_N(t_i-t_j)\overline{D'_N(t_{i'}-t_{j'})}\mathbb{E}[(\delta_j\epsilon_i+\epsilon_j^2\delta_i+\epsilon_j^2\epsilon_i+2\delta_j\delta_i\epsilon_j+2\delta_j\epsilon_i\epsilon_j) \\ & (\delta_{j'}\epsilon_{i'}+\epsilon_{j'}^2\delta_{i'}+\epsilon_{j'}^2\epsilon_{i'}+2\delta_{j'}\delta_{i'}\epsilon_{j'}+2\delta_{j'}\epsilon_{i'}\epsilon_{j'})]. \end{aligned} \quad (55)$$

Under Assumption (H2), we have that (53) is equal to

$$\sum_{i,j} (D'_N(t_i - t_j))^2 (\mathbb{E}[\delta_j^2] \mathbb{E}[\epsilon_i^2] + \mathbb{E}[\epsilon_j^4] \mathbb{E}[\delta_i^2] + \mathbb{E}[\epsilon_j^4 \epsilon_i^2] + 4\mathbb{E}[\delta_j^2 \delta_i^2] \mathbb{E}[\epsilon_j^2] + 4\mathbb{E}[\delta_j^2] \mathbb{E}[\epsilon_i^2 \epsilon_j^2]) \quad (56)$$

$$+ \sum_{i,j,i',j':i \neq i', j \neq j'} D'_N(t_i - t_j) \overline{D'_N(t_{i'} - t_{j'})} \mathbb{E}[\epsilon_j^2 \epsilon_i \epsilon_{j'}^2 \epsilon_{i'}]. \quad (57)$$

It holds that

$$\mathbb{E}[\epsilon_i^2] = 2\mathbb{E}[\zeta^2]$$

$$\mathbb{E}[\epsilon_i^4] = 2\mathbb{E}[\zeta^4] + 6\mathbb{E}[\zeta^2]^2$$

$$\mathbb{E}[\epsilon_j^4 \epsilon_i^2] = \begin{cases} 4\mathbb{E}[\zeta^4] \mathbb{E}[\zeta^2] + 12\mathbb{E}[\zeta^2]^3 & \text{if } |i - j| \neq 1, \\ 9\mathbb{E}[\zeta^4] \mathbb{E}[\zeta^2] + \mathbb{E}[\zeta^6] + 6\mathbb{E}[\zeta^2]^3 - 4\mathbb{E}[\zeta^3]^2 & \text{if } i = j - 1, \\ 13\mathbb{E}[\zeta^4] \mathbb{E}[\zeta^2] + \mathbb{E}[\zeta^6] + 2\mathbb{E}[\zeta^2]^3 - 4\mathbb{E}[\zeta^3]^2 & \text{if } i = j + 1. \end{cases}$$

$$\mathbb{E}[\epsilon_j^2 \epsilon_i^2] = \begin{cases} 4\mathbb{E}[\zeta^2]^2 & \text{if } |i - j| > 1, \\ 3\mathbb{E}[\zeta^2]^2 + \mathbb{E}[\zeta^4] & \text{if } i = j - 1, \\ 3\mathbb{E}[\zeta^2]^2 + \mathbb{E}[\zeta^4] & \text{if } i = j + 1. \end{cases}$$

$$\mathbb{E}[\epsilon_i^3] = 0$$

$$\mathbb{E}[\epsilon_j^2 \epsilon_i \epsilon_{j'}^2 \epsilon_{i'}] = \begin{cases} 0 & \text{if } i \neq i', j \neq j', i \neq j', j \neq i', \\ 0 & \text{if } i \neq i', j \neq j', i = j', j = i' \text{ and } |i - j| \neq 1, \\ \mathbb{E}[\zeta^3]^2 - \mathbb{E}[\zeta^6] - 6\mathbb{E}[\zeta^4] \mathbb{E}[\zeta^2] - 9\mathbb{E}[\zeta^2]^3 & \text{if } i \neq i', j \neq j', i = j', j = i' \text{ and } i = j + 1, \\ \mathbb{E}[\zeta^3]^2 - \mathbb{E}[\zeta^6] - 6\mathbb{E}[\zeta^4] \mathbb{E}[\zeta^2] - 9\mathbb{E}[\zeta^2]^3 & \text{if } i \neq i', j \neq j', i = j', j = i' \text{ and } i = j - 1. \end{cases}$$

Therefore (53) is equal to

$$\sum_{i,j} (D'_N(t_i - t_j))^2 (2\mathbb{E}[\delta_j^2]\mathbb{E}[\zeta^2] + 2\mathbb{E}[\delta_i^2]\mathbb{E}[\zeta^4] + 6\mathbb{E}[\delta_i^2]\mathbb{E}[\zeta^2]^2 + 8\mathbb{E}[\delta_i^2\delta_j^2]\mathbb{E}[\zeta^2]) \quad (58)$$

$$+ \sum_{i,j:|i-j|\neq 1} (D'_N(t_i - t_j))^2 16\mathbb{E}[\delta_j^2]\mathbb{E}[\zeta^2]^2 + \sum_{i,j:|i-j|=1} (D'_N(t_i - t_j))^2 \mathbb{E}[\delta_j^2] (12\mathbb{E}[\zeta^2]^2 + 4\mathbb{E}[\zeta^4]) \quad (59)$$

$$+ \sum_{i,j:|i-j|\neq 1} (D'_N(t_i - t_j))^2 (4\mathbb{E}[\zeta^4]\mathbb{E}[\zeta^2] + 12\mathbb{E}[\zeta^2]^3) \quad (60)$$

$$+ \sum_{i,j:i=j-1} (D'_N(t_{j-1} - t_j))^2 (9\mathbb{E}[\zeta^4]\mathbb{E}[\zeta^2] + \mathbb{E}[\zeta^6] + 6\mathbb{E}[\zeta^2]^3 - 4\mathbb{E}[\zeta^3]^2) \quad (61)$$

$$+ \sum_{i,j:i=j+1} (D'_N(t_{j+1} - t_j))^2 (13\mathbb{E}[\zeta^4]\mathbb{E}[\zeta^2] + \mathbb{E}[\zeta^6] + 2\mathbb{E}[\zeta^2]^3 - 4\mathbb{E}[\zeta^3]^2) \quad (62)$$

$$+ \sum_{i,j:i=j-1} D'_N(t_{j-1} - t_j) \overline{D'_N(t_j - t_{j-1})} (\mathbb{E}[\zeta^3]^2 - \mathbb{E}[\zeta^6] - 6\mathbb{E}[\zeta^4]\mathbb{E}[\zeta^2] - 9\mathbb{E}[\zeta^2]^3) \quad (63)$$

$$+ \sum_{i,j:i=j+1} D'_N(t_{j+1} - t_j) \overline{D'_N(t_j - t_{j+1})} (\mathbb{E}[\zeta^3]^2 - \mathbb{E}[\zeta^6] - 6\mathbb{E}[\zeta^4]\mathbb{E}[\zeta^2] - 9\mathbb{E}[\zeta^2]^3) \quad (64)$$

Computing the summands from (61) to (64), we obtain

$$(n-1) \left(\frac{1}{(2N+1)^2} \sum_{|l|<N} l^2 \frac{4\pi^2}{T^2} + \frac{1}{(2N+1)^2} \sum_{l \neq l'} l l' \frac{4\pi^2}{T^2} e^{-i\frac{2\pi}{n}(l-l')} \right) \\ \times (9\mathbb{E}[\zeta^4]\mathbb{E}[\zeta^2] + \mathbb{E}[\zeta^6] + 6\mathbb{E}[\zeta^2]^3 - 4\mathbb{E}[\zeta^3]^2) \quad (65)$$

$$+(n-1) \left(\frac{1}{(2N+1)^2} \sum_{|l|<N} l^2 \frac{4\pi^2}{T^2} + \frac{1}{(2N+1)^2} \sum_{l \neq l'} l l' \frac{4\pi^2}{T^2} e^{i\frac{2\pi}{n}(l-l')} \right) \\ \times (13\mathbb{E}[\zeta^4]\mathbb{E}[\zeta^2] + \mathbb{E}[\zeta^6] + 2\mathbb{E}[\zeta^2]^3 - 4\mathbb{E}[\zeta^3]^2) \quad (66)$$

$$+(n-1) \left(\frac{1}{(2N+1)^2} \sum_{|l|<N} l^2 \frac{4\pi^2}{T^2} e^{-i\frac{4\pi}{n}l} + \frac{1}{(2N+1)^2} \sum_{l \neq l'} l l' \frac{4\pi^2}{T^2} e^{-i\frac{2\pi}{n}(l'+l)} \right) \\ \times (\mathbb{E}[\zeta^3]^2 - \mathbb{E}[\zeta^6] - 6\mathbb{E}[\zeta^4]\mathbb{E}[\zeta^2] - 9\mathbb{E}[\zeta^2]^3) \quad (67)$$

$$+(n-1) \left(\frac{1}{(2N+1)^2} \sum_{|l|<N} l^2 \frac{4\pi^2}{T^2} e^{+i\frac{4\pi}{n}l} + \frac{1}{(2N+1)^2} \sum_{l \neq l'} l l' \frac{4\pi^2}{T^2} e^{i\frac{2\pi}{n}(l'+l)} \right) \\ \times (\mathbb{E}[\zeta^3]^2 - \mathbb{E}[\zeta^6] - 6\mathbb{E}[\zeta^4]\mathbb{E}[\zeta^2] - 9\mathbb{E}[\zeta^2]^3) \quad (68)$$

The terms where the indices l and l' appear in (65) and (67) has to be summed up following the rule highlighted in Table 7. The same applies for the terms where the indices l and l' appear in (66) and (68).

Indices belonging to (65)	Indices belonging to (67)
$l > 0, l' > 0$	$l > 0, l' < 0$
$l < 0, l' < 0$	$l < 0, l' > 0$
$l > 0, l' < 0$	$l > 0, l' > 0$
$l < 0, l' > 0$	$l < 0, l' < 0$

Table 7: Summing rule: the terms has to be first summed according to the indices present in each row, then the resulting addends has to be summed with respect to the indices grouped by color.

The summands from (61) to (64) are then equal to

$$(n-1) \frac{1}{(2N+1)^2} \sum_{|l| < N} l^2 \frac{4\pi^2}{T^2} (22\mathbb{E}[\zeta^4]\mathbb{E}[\zeta^2] + 2\mathbb{E}[\zeta^6] + 8\mathbb{E}[\zeta^2]^3 - 8\mathbb{E}[\zeta^3]^2) \quad (69)$$

$$+ (n-1) \frac{1}{(2N+1)^2} \sum_{|l| < N} l^2 \frac{4\pi^2}{T^2} 2 \cos\left(\frac{4\pi}{n}l\right) (\mathbb{E}[\zeta^3]^2 - \mathbb{E}[\zeta^6] - 6\mathbb{E}[\zeta^4]\mathbb{E}[\zeta^2] - 9\mathbb{E}[\zeta^2]^3) \quad (70)$$

$$+ (n-1) \frac{1}{(2N+1)^2} \sum_{l, l' > 0} ll' \frac{4\pi^2}{T^2} \sin\left(\frac{2\pi}{n}l\right) \sin\left(\frac{2\pi}{n}l'\right) (34\mathbb{E}[\zeta^4]\mathbb{E}[\zeta^2] + 4\mathbb{E}[\zeta^6] + 26\mathbb{E}[\zeta^2]^3 - 5\mathbb{E}[\zeta^3]^2). \quad (71)$$

If $N = n^{\frac{1}{\beta}}$ with $\beta > \frac{\log(n)}{\log(n)-\log(8)}$ then $0 \leq \cos\left(\frac{4\pi}{n}l\right) \leq 1$ for all $|l| \leq N$. If $\beta > \frac{\log(n)}{\log(n)-\log(2)}$ then $0 \leq \sin\left(\frac{2\pi}{n}l\right) \leq 1$. We have that the choice of $\beta > \frac{\log(n)}{\log(n)-\log(8)}$ is implied by the ratio in (29). In conclusion, the term (71) is greater than or equal to zero and the sum between (69) and (70) is greater than or equal to

$$(n-1) \frac{1}{(2N+1)^2} \sum_{|l| < N} l^2 \frac{4\pi^2}{T^2} (22\mathbb{E}[\zeta^4]\mathbb{E}[\zeta^2] + 2\mathbb{E}[\zeta^6] + 8\mathbb{E}[\zeta^2]^3 - 8\mathbb{E}[\zeta^3]^2), \quad (72)$$

if $(\mathbb{E}[\zeta^3]^2 - \mathbb{E}[\zeta^6] - 6\mathbb{E}[\zeta^4]\mathbb{E}[\zeta^2] - 9\mathbb{E}[\zeta^2]^3) > 0$ and greater than or equal to

$$(n-1) \frac{1}{(2N+1)^2} \sum_{|l| < N} l^2 \frac{4\pi^2}{T^2} (10\mathbb{E}[\zeta^4]\mathbb{E}[\zeta^2] - 10\mathbb{E}[\zeta^2]^3 - 6\mathbb{E}[\zeta^3]^2), \quad (73)$$

if $(\mathbb{E}[\zeta^3]^2 - \mathbb{E}[\zeta^6] - 6\mathbb{E}[\zeta^4]\mathbb{E}[\zeta^2] - 9\mathbb{E}[\zeta^2]^3) < 0$.

Let us now analyse the summands from (58) to (60). They are equal to

	l, l'	$-l, -l'$
s	$ll'(\cos(2\pi/n(ls - l's)) + i \sin(2\pi/n(ls - l's)))$	$ll'(\cos(2\pi/n(-ls + l's)) + i \sin(2\pi/n(-ls + l's)))$
$-s$	$ll'(\cos(2\pi/n(-ls + l's)) + i \sin(2\pi/n(-ls + l's)))$	$ll'(\cos(2\pi/n(ls - l's)) + i \sin(2\pi/n(ls - l's)))$
	$l, -l'$	$-l, l'$
s	$-ll'(\cos(2\pi/n(ls + l's)) + i \sin(2\pi/n(ls + l's)))$	$-ll'(\cos(2\pi/n(-ls - l's)) + i \sin(2\pi/n(-ls - l's)))$
$-s$	$-ll'(\cos(2\pi/n(-ls - l's)) + i \sin(2\pi/n(-ls - l's)))$	$-ll'(\cos(2\pi/n(ls + l's)) + i \sin(2\pi/n(ls + l's)))$

Table 8: Coefficients appearing in the summands from (74) to (77) with respect to the indices l, l', s . Note that $t_i - t_j = \frac{2\pi}{n}s$ and all the indices are considered positive constants.

	l, l'
s	$ll'(2 \cos(2\pi/n(ls - l's)))$
$-s$	$ll'(2 \cos(2\pi/n(-ls + l's)))$
	$l, -l'$
s	$-ll'(2 \cos(2\pi/n(ls + l's)))$
$-s$	$-ll'(2 \cos(2\pi/n(-ls - l's)))$

Table 9: Coefficients appearing in the summands from (74) to (77) with respect to the indices l, l', s . Note that $t_i - t_j = \frac{2\pi}{n}s$ and all the indices are considered positive constants.

$$\sum_{i,j} \left(\frac{1}{(2N+1)^2} \sum_{|l|<N} l^2 \frac{4\pi^2}{T^2} + \frac{1}{(2N+1)^2} \sum_{l \neq l'} ll' \frac{4\pi^2}{T^2} e^{-i\frac{2\pi}{T}(l-l')(t_i-t_j)} \right) \times (2\mathbb{E}[\delta_j^2]\mathbb{E}[\zeta^2] + 2\mathbb{E}[\delta_i^2]\mathbb{E}[\zeta^4] + 6\mathbb{E}[\delta_i^2]\mathbb{E}[\zeta^2]^2 + 8\mathbb{E}[\delta_i^2\delta_j^2]\mathbb{E}[\zeta^2]) \quad (74)$$

$$+ \sum_{i,j:|i-j| \neq 1} \left(\frac{1}{(2N+1)^2} \sum_{|l|<N} l^2 \frac{4\pi^2}{T^2} + \frac{1}{(2N+1)^2} \sum_{l \neq l'} ll' \frac{4\pi^2}{T^2} e^{-i\frac{2\pi}{T}(l-l')(t_i-t_j)} \right) 16\mathbb{E}[\delta_j^2]\mathbb{E}[\zeta^2]^2 \quad (75)$$

$$+ \sum_{i,j:|i-j|=1} \left(\frac{1}{(2N+1)^2} \sum_{|l|<N} l^2 \frac{4\pi^2}{T^2} + \frac{1}{(2N+1)^2} \sum_{l \neq l'} ll' \frac{4\pi^2}{T^2} e^{-i\frac{2\pi}{T}(l-l')(t_i-t_j)} \right) \mathbb{E}[\delta_j^2](12\mathbb{E}[\zeta^2]^2 + 4\mathbb{E}[\zeta^4]) \quad (76)$$

$$+ \sum_{i,j:|i-j| \neq 1} \left(\frac{1}{(2N+1)^2} \sum_{|l|<N} l^2 \frac{4\pi^2}{T^2} + \frac{1}{(2N+1)^2} \sum_{l \neq l'} ll' \frac{4\pi^2}{T^2} e^{-i\frac{2\pi}{T}(l-l')(t_i-t_j)} \right) (4\mathbb{E}[\zeta^4]\mathbb{E}[\zeta^2] + 12\mathbb{E}[\zeta^2]^3). \quad (77)$$

We first take care of the sum with respect to the indices i, j, l and l' appearing in the terms (74) to (77). To simply explain the calculations below, let us consider from now on that the indices l and l' are positive and that there exists an $s = 1, \dots, n-1$ such that if $t_i > t_j$, $t_i - t_j = s\frac{2\pi}{n}$. We do not consider $s = 0$ in the calculations below because $D'_N(t_i - t_i) = 0$. In Table 8, we find, for fixed values of s, l, l' , all the possible combination of the indices and the expression of the terms $ll'e^{-i\frac{2\pi}{T}(l-l')(t_i-t_j)}$ appearing in the summands. The blue and the red elements appear in (74), (75), (76) and (77), respectively, the same number of times. We first sum each row of Table 8. We then obtain, Table 9. Summing up the blue and red terms obtained for s and $-s$, respectively, we have

$$\sum_{i,j} \frac{1}{(2N+1)^2} \sum_{|l|<N} l^2 \frac{4\pi^2}{T^2} (2\mathbb{E}[\delta_j^2]\mathbb{E}[\zeta^2] + 2\mathbb{E}[\delta_i^2]\mathbb{E}[\zeta^4] + 6\mathbb{E}[\delta_i^2]\mathbb{E}[\zeta^2]^2 + 8\mathbb{E}[\delta_i^2\delta_j^2]\mathbb{E}[\zeta^2]) \quad (78)$$

$$\begin{aligned} & \sum_{i=1}^{n-1} \sum_{j=0}^{i-1} \frac{1}{(2N+1)^2} \sum_{l,l'>0} ll' \frac{4\pi^2}{T^2} 4 \sin\left(\frac{2\pi}{n}ls\right) \sin\left(\frac{2\pi}{n}l's\right) \\ & \times (2\mathbb{E}[\delta_j^2]\mathbb{E}[\zeta^2] + 2\mathbb{E}[\delta_i^2]\mathbb{E}[\zeta^4] + 6\mathbb{E}[\delta_i^2]\mathbb{E}[\zeta^2]^2 + 8\mathbb{E}[\delta_i^2\delta_j^2]\mathbb{E}[\zeta^2]) \end{aligned} \quad (79)$$

$$+ \sum_{i,j:|i-j|\neq 1} \frac{1}{(2N+1)^2} \sum_{|l|<N} l^2 \frac{4\pi^2}{T^2} 16\mathbb{E}[\delta_j^2]\mathbb{E}[\zeta^2]^2 \quad (80)$$

$$+ \sum_{i=2}^{n-1} \sum_{j=0}^{i-2} \frac{1}{(2N+1)^2} \sum_{l,l'>0} ll' \frac{4\pi^2}{T^2} 4 \sin\left(\frac{2\pi}{n}ls\right) \sin\left(\frac{2\pi}{n}l's\right) 16\mathbb{E}[\delta_j^2]\mathbb{E}[\zeta^2]^2 \quad (81)$$

$$+ \sum_{i,j:|i-j|=1} \frac{1}{(2N+1)^2} \sum_{|l|<N} l^2 \frac{4\pi^2}{T^2} \mathbb{E}[\delta_j^2] (12\mathbb{E}[\zeta^2]^2 + 4\mathbb{E}[\zeta^4]) \quad (82)$$

$$+ (n-1) \frac{1}{(2N+1)^2} \sum_{l,l'>0} ll' \frac{4\pi^2}{T^2} 4 \sin\left(\frac{2\pi}{n}l\right) \sin\left(\frac{2\pi}{n}l'\right) \mathbb{E}[\delta_j^2] (12\mathbb{E}[\zeta^2]^2 + 4\mathbb{E}[\zeta^4]) \quad (83)$$

$$+ \sum_{i,j:|i-j|\neq 1} \frac{1}{(2N+1)^2} \sum_{|l|<N} l^2 \frac{4\pi^2}{T^2} (4\mathbb{E}[\zeta^4]\mathbb{E}[\zeta^2] + 12\mathbb{E}[\zeta^2]^3) \quad (84)$$

$$+ \sum_{i=2}^{n-1} \sum_{j=0}^{i-2} \frac{1}{(2N+1)^2} \sum_{l,l'>0} ll' \frac{4\pi^2}{T^2} 4 \sin\left(\frac{2\pi}{n}ls\right) \sin\left(\frac{2\pi}{n}l's\right) (4\mathbb{E}[\zeta^4]\mathbb{E}[\zeta^2] + 12\mathbb{E}[\zeta^2]^3) \quad (85)$$

If $N = n^{\frac{1}{\beta}}$ such that $\beta > \frac{\log(n)}{\log(n) - \log(2(n-1))}$ then $0 \leq \sin\left(\frac{2\pi}{n}ls\right) \leq 1$ for $s = 1, \dots, n-1$ and $l > 0$. The latter is straightforwardly implied by (29), being $\frac{\log(n)}{\log(n) - \log(2(n-1))}$ negative. Therefore, the summands (79), (81), (83) and (85) are greater than or equal to zero.

In conclusion, (53) is possibly greater than or equal to two sums. The first one is

$$\begin{aligned} & \sum_{i,j} \frac{1}{(2N+1)^2} \sum_{|l|<N} l^2 \frac{4\pi^2}{T^2} (2\mathbb{E}[\delta_j^2]\mathbb{E}[\zeta^2] + 2\mathbb{E}[\delta_i^2]\mathbb{E}[\zeta^4] + 6\mathbb{E}[\delta_i^2]\mathbb{E}[\zeta^2]^2 + 8\mathbb{E}[\delta_i^2\delta_j^2]\mathbb{E}[\zeta^2]) \\ & + \sum_{i,j:|i-j|\neq 1} \frac{1}{(2N+1)^2} \sum_{|l|<N} l^2 \frac{4\pi^2}{T^2} 16\mathbb{E}[\delta_j^2]\mathbb{E}[\zeta^2]^2 \\ & + \sum_{i,j:|i-j|=1} \frac{1}{(2N+1)^2} \sum_{|l|<N} l^2 \frac{4\pi^2}{T^2} \mathbb{E}[\delta_j^2] (12\mathbb{E}[\zeta^2]^2 + 4\mathbb{E}[\zeta^4]) \\ & + \sum_{i,j:|i-j|\neq 1} \frac{1}{(2N+1)^2} \sum_{|l|<N} l^2 \frac{4\pi^2}{T^2} (4\mathbb{E}[\zeta^4]\mathbb{E}[\zeta^2] + 12\mathbb{E}[\zeta^2]^3) \\ & + (n-1) \frac{1}{(2N+1)^2} \sum_{|l|<N} l^2 \frac{4\pi^2}{T^2} (22\mathbb{E}[\zeta^4]\mathbb{E}[\zeta^2] + 2\mathbb{E}[\zeta^6] + 8\mathbb{E}[\zeta^2]^3 - 8\mathbb{E}[\zeta^3]^2), \end{aligned} \quad (86)$$

and the second one is

$$\begin{aligned}
& \sum_{i,j} \frac{1}{(2N+1)^2} \sum_{|l|<N} l^2 \frac{4\pi^2}{T^2} (2\mathbb{E}[\delta_j^2]\mathbb{E}[\zeta^2] + 2\mathbb{E}[\delta_i^2]\mathbb{E}[\zeta^4] + 6\mathbb{E}[\delta_i^2]\mathbb{E}[\zeta^2]^2 + 8\mathbb{E}[\delta_i^2\delta_j^2]\mathbb{E}[\zeta^2]) \\
& + \sum_{i,j:|i-j|\neq 1} \frac{1}{(2N+1)^2} \sum_{|l|<N} l^2 \frac{4\pi^2}{T^2} 16\mathbb{E}[\delta_j^2]\mathbb{E}[\zeta^2]^2 \\
& \quad + \sum_{i,j:|i-j|=1} \frac{1}{(2N+1)^2} \sum_{|l|<N} l^2 \frac{4\pi^2}{T^2} \mathbb{E}[\delta_j^2](12\mathbb{E}[\zeta^2]^2 + 4\mathbb{E}[\zeta^4]) \\
& + \sum_{i,j:|i-j|\neq 1} \frac{1}{(2N+1)^2} \sum_{|l|<N} l^2 \frac{4\pi^2}{T^2} (4\mathbb{E}[\zeta^4]\mathbb{E}[\zeta^2] + 12\mathbb{E}[\zeta^2]^3) \\
& + (n-1) \frac{1}{(2N+1)^2} \sum_{|l|<N} l^2 \frac{4\pi^2}{T^2} (10\mathbb{E}[\zeta^4]\mathbb{E}[\zeta^2] - 10\mathbb{E}[\zeta^2]^3 - 6\mathbb{E}[\zeta^3]^2).
\end{aligned} \tag{87}$$

Note that because of Assumption (H1), the terms $\mathbb{E}[\delta_i^2]$ and $\mathbb{E}[\delta_i^2\delta_j^2]$ are positive and finite constants. The behaviour of the sums (86) and (87) is ruled by their first summands. In fact,

$$\sum_{i,j} \frac{1}{(2N+1)^2} \sum_{|l|\leq N} l^2 \frac{4\pi^2}{T^2} = \frac{n^2}{(2N+1)^2} \frac{4\pi^2}{T^2} \left(\frac{N^3}{3} + \frac{N^2}{2} + \frac{N}{6} \right),$$

which diverges as $n, N \rightarrow \infty$. ■

References

- [1] Y. Ait-Sahalia, J. Fan, R. Laeven, D. Wang, and X. Yang, The estimation of continuous and discontinuous leverage effects, *Journal of the American Statistical Association* 112, (2017), 1744–1758.
- [2] Y. Ait-Sahalia, J. Fan and Y. Li, The leverage effect puzzle: Disentangling sources of bias at high-frequency, *Journal of Financial Economics* 109 (2013), 224–249.
- [3] Y. Ait-Sahalia and J. Jacod, *High-Frequency Financial Econometrics*, Princeton University Press, 2014.
- [4] F. Bandi and R. Renò, Time-varying leverage effects, *Journal of Econometrics* 169 (1) (2012), 94–113.
- [5] F. M Bandi and J. R. Russell, Microstructure Noise, Realized Variance, and Optimal Sampling, *The Review of Economic Studies*, 75 (2) (2008), 339–369.

- [6] E. Barucci and M. E. Mancino, Computation of volatility in stochastic volatility models with high-frequency data, *International journal of theoretical and applied finance* 13 (5) (2010), 767–787.
- [7] G. Bekaert and G. Wu, Asymmetric volatility and risk in equity markets, *The Review of Financial Studies* 13 (2000), 1–42.
- [8] F. Black, Studies of stock market volatility changes, *Proceedings of the Business and Economic Statistic Section, American Statistical Association* (1976), 177–181.
- [9] T. Bollerslev, J. Litvinova and G. Tauchen, Leverage and volatility feedback effects in high-frequency data, *Journal of Financial Econometrics* 4 (3) (2006), 353–384.
- [10] J. Y. Campbell. Stock returns and the term structure, *Journal of Financial Economics* 18 (2) (1987), 373–399.
- [11] J. Y., Campbell and L. Hentschel, No news is good news: an asymmetric model of changing volatility in stock returns, *Journal of Financial Economics* 31 (1992), 281–331.
- [12] P. Carr and L. Wu, Stochastic skew in currency options, *Journal of Financial Econometrics* 86 (1) (2007), 213–247.
- [13] K. Christensen, R. C. A. Oomen and M. Podolskij, Fact or friction:jumps at ultra high-frequency, *Journal of Financial Economics*, 114 (2014), 576–599.
- [14] A. A. Christie, The stochastic behavior of common stock variances, *Journal of Financial Econometrics* 10 (1982), 407–432.
- [15] I. V. Curato, Estimation of the stochastic leverage effect using the Fourier transform method, *Stochastic Processes and their Applications* 129 (2019), 3207–3238.
- [16] I. V. Curato and S. Sanfelici, Measuring the leverage effect in a high-frequency trading framework, *Handbook of high-frequency Trading*, G.N. Gregoriou Ed., Elsevier, Plattsburgh, NY, USA (2015), 425–446.
- [17] K. R. French, G. W. Schwert and R. F. Stambaugh, Expected Stock Returns and Volatility, *Journal of Financial Economics* 19 (1987), 3–30.
- [18] S. Figlewski and X. Wang, Is the leverage effect a leverage effect?, Working Paper, Department of Finance, New York University (2001).
- [19] E. Ghysel, P. Santa-Clara and R. Valkanov, There is a risk-return tradeoff after all, *Journal of Financial Econometrics* 2 (2005), 177–210.
- [20] P. Glasserman, *Monte Carlo Methods in Financial Engineering*, Springer Science & Business Media, (2004).

- [21] S. Heston, A closed-form solution for options with stochastic volatility with applications to bond and currency options, *Review of Financial Studies* 6 (1993), 327–344.
- [22] I. Kalnina and D. Xiu, Nonparametric Estimation of the Leverage Effect: A Trade-Off Between Robustness and Efficiency. *Journal of the American Statistical Association* 112 (2017), 384–396.
- [23] J. Jacod, Y. Li, P. A. Mykland, M. Podolskij and M. Vetter, Microstructure Noise in the Continuous Case: The Pre-Averaging Approach, *Stochastic Processes and Their Applications*, 119 (2009), 2249–2276.
- [24] P. Malliavin and M. E. Mancino, Fourier series method for measurement of multivariate volatilities, *Finance and Stochastics* 4 (2002), 49–61.
- [25] Malliavin, P. and Mancino, M. E. , A Fourier transform method for nonparametric estimation of volatility, *The Annals of Statistics* 37 (4) (2009), 1983–2010.
- [26] M. E. Mancino, M.C. Recchioni and S. Sanfelici, *Fourier-Malliavin Volatility Estimation: theory and practice*, Springer Briefs in Quantitative Finance, (2017).
- [27] M.E. Mancino and S. Sanfelici, Robustness of Fourier estimator of integrated volatility in the presence of microstructure noise, *Computational statistics and data analysis* 52 (6) (2008), 2966–2989.
- [28] M. E. Mancino and G. Toscano. Rate Efficient Asymptotic Normality for the Fourier Estimator of the Leverage Process (2020), Working paper.
- [29] P. A. Mykland and D. Wang, The estimation of leverage effect with high-frequency data, *Journal of the American Statistical Association* 109 (505) (2012), 197–215 .
- [30] P. A. Mykland and L. Zhang, Inference for continuous semimartingales observed at high frequency, *Econometrica* 77 (2009), 1403–1455.
- [31] D. B. Nelson, Conditional heteroskedasticity in asset returns: a new approach, *Econometrica* 59 (2) (1991), 347–370.
- [32] S. Sanfelici, I.V. Curato and M.E. Mancino, High-frequency volatility of volatility estimation free from spot volatility estimates, *Quantitative Finance* 15 (8) (2015), 1331–1345.
- [33] G. Tauchen, H. Zhang and M. Liu, Volume, volatility and leverage: a dynamic analysis, *Journal of Econometrics* 74 (1) (1996), 177–208.
- [34] Vetter, M., Estimation of integrated volatility of volatility with applications to goodness-of-fit testing, *Bernoulli* 21 (4) (2015), 2393–2418.

- [35] A. E. D. Veraart and L. A. M. Veraart, Stochastic volatility and stochastic leverage, *Annals of Finance* 8 (2012), 205–233.
- [36] G. Wu, The determinants of asymmetric volatility, *Review of Financial Studies* 14 (2001), 837–859.
- [37] J. Yu, A semiparametric stochastic volatility model, *Journal of Econometrics*, 167(2) (2012), 473–482.